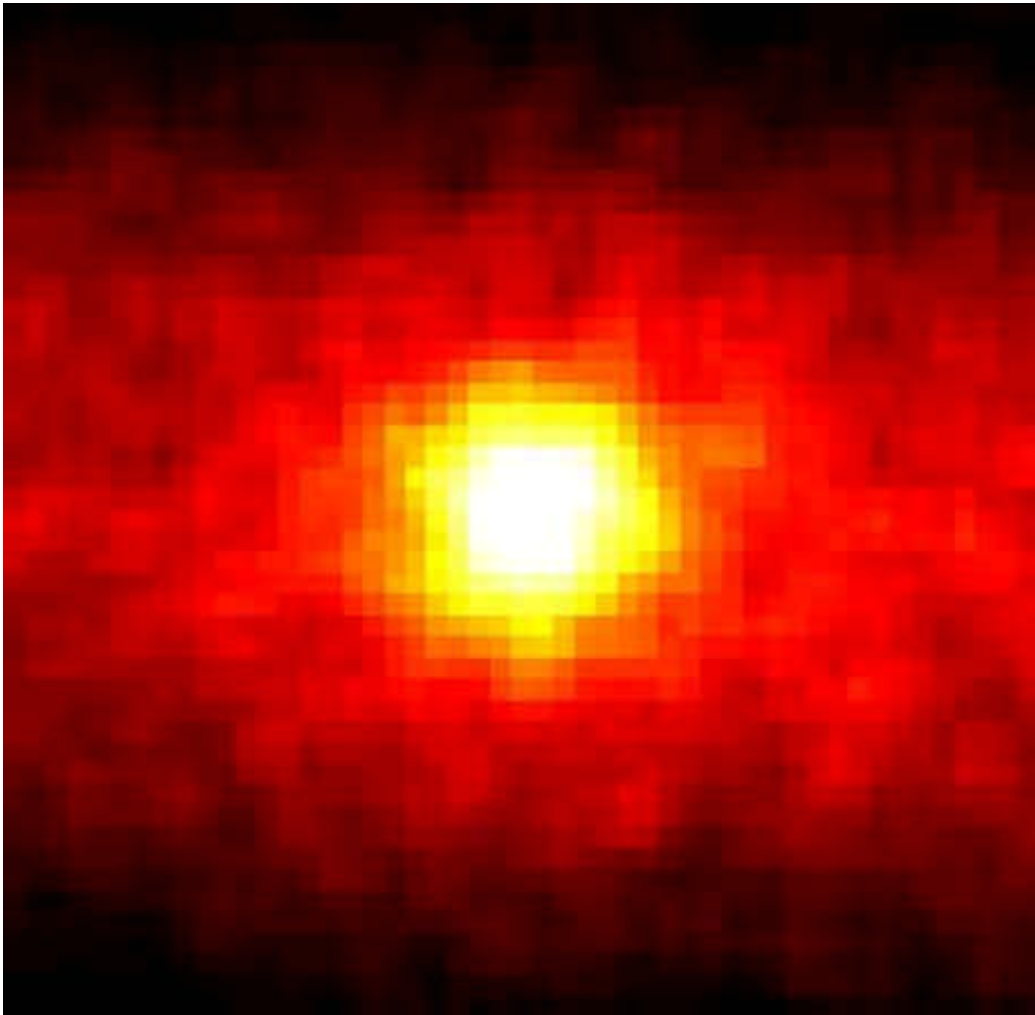
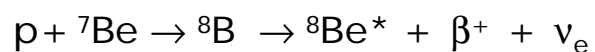


## Neutrino image of the sun by Super-K



- 500 days of data from Super-K
- picture covers 90x90 degrees in R.A. and Dec.
- The core of the sun emits neutrinos from fusion reactions.
- Nearly all solar neutrinos *detected here* are produced by



The astrophysical S-factor for  ${}^7\text{Be} + \text{p} \Rightarrow {}^8\text{B}$   
and implications for solar neutrino physics

Summer Nuclear Institute at TRIUMF 2002

The  ${}^7\text{Be}(\text{p},\gamma){}^8\text{B}$  reaction and solar neutrinos

Kurt Snover  
Univ. Washington  
Seattle

Outline:

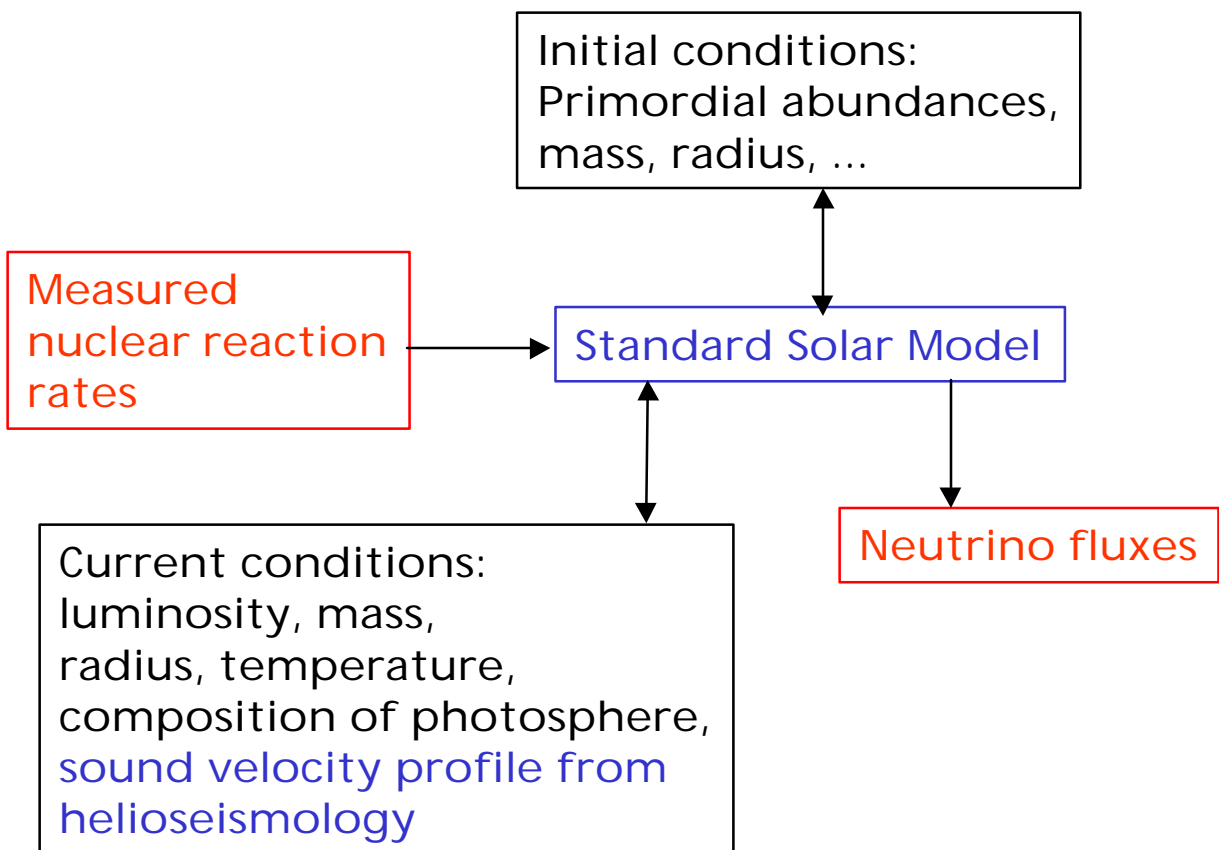
- I. Introduction and motivation
- II. Solar model
- III. The  ${}^7\text{Be}(\text{p},\gamma){}^8\text{B}$  reaction
- IV. Implications for neutrino physics

## Bibliography/Reading list

- Clayton, Donald R., Principles of Stellar Evolution and Nucleosynthesis, McGraw Hill, 1968.
- Bahcall, J.N., Neutrino Astrophysics, Cambridge Univ. Press, 1989; <http://www.sns.ias.edu/~jnb/>
- Rofcs, C.E. and Rodney, W.S., Cauldrons in the Cosmos, Univ of Chicago Press, 1988.
- Langanke, K., and Barnes, C.A., Nucleosynthesis in the Big Bang and in Stars, Adv. In Nucl. Phys. Vol. 22, Chapt. 5.
- Klapdor-Kleingrothaus, H.V., and Zuber, K., Particle Astrophysics (revised edition), IOP Publishing, 2000.
- Celebrating the neutrino, Los Alamos Science, vol. 25.
- Adelberger, E.G., et. Al., Solar Fusion Cross sections, Rev. Mod. Phys. 70, 1265 (1998).
- Junghans, A.R., et. Al.,  ${}^7\text{Be}(p,\gamma){}^8\text{B}$  astrophysical S-factor from precision cross section measurements, Phys. Rev. Lett. 88, 041101-1(2002) and references therein.

## The Standard Solar Model (Bahcall)

- spherical, (initially) homogenous, nonrotating
- hydrostatic equilibrium between gravity and radiation + particle pressure
- energy transport by radiation and convection
- energy generation by nuclear reactions
- chemical and isotopic abundance changes only by nuclear reactions



## Some interesting facts about our Sun:

- age =  $4.6 \times 10^9$  years

- Composition:

Hydrogen	Helium	Metals( $Z > 2$ )	time
71%	27%	2%	birth
34%	64%	2%	now

- core temperature =  $15.6 \times 10^6$  K,  $kT_{\text{core}} = 1.3$  keV

- core density  $\cong 156$  g/cm<sup>3</sup>

- core hydrogen density  $\cong 0.5$  x surface hydrogen density

- interior is fully ionized and nearly an ideal gas

- time for a photon to diffuse from the center to the surface is  $\sim 10^4$  years

- fraction of energy from p-p cycle: 98.4%;  
from CNO cycle: 1.6%.

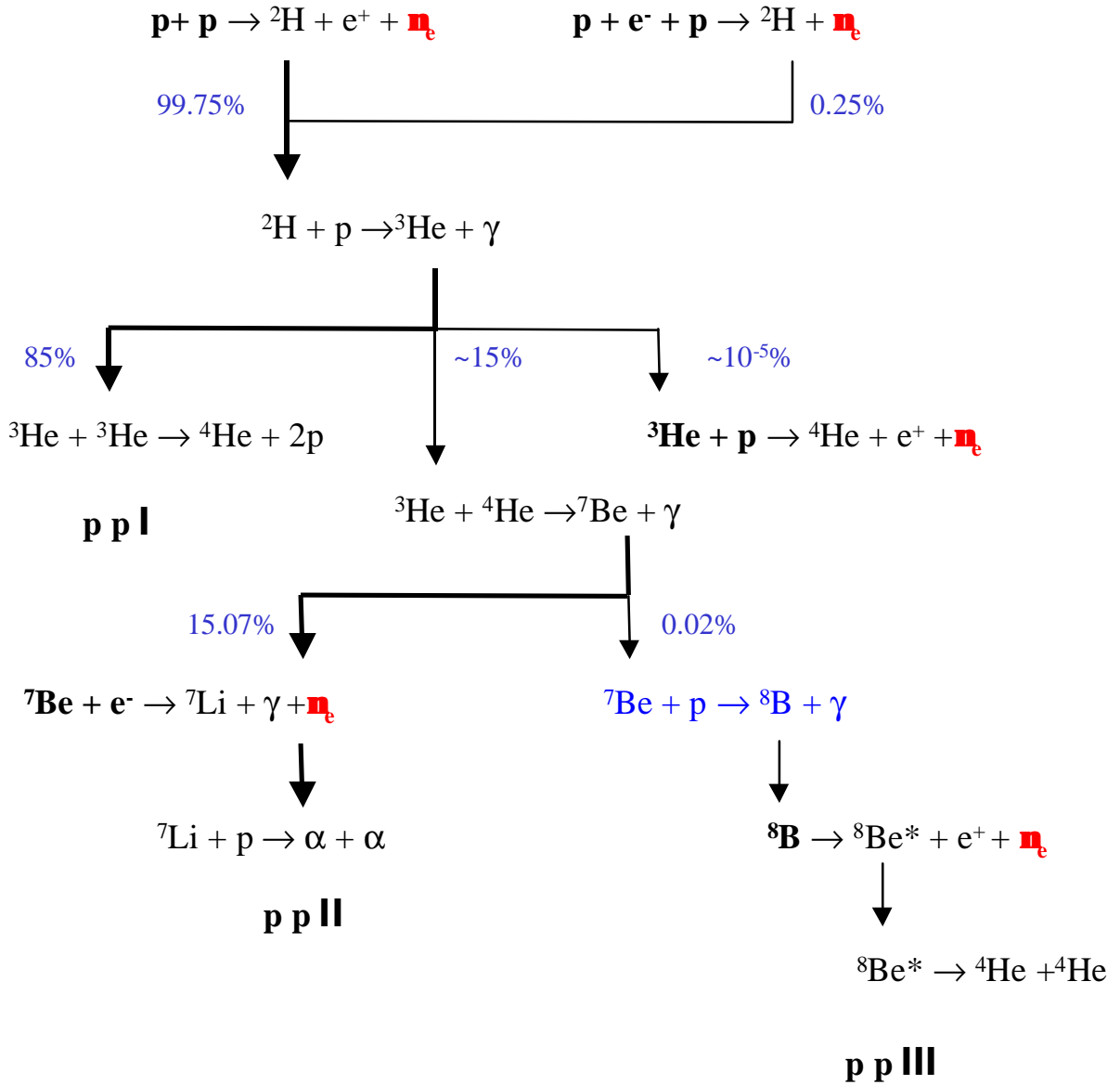
- over the life of the sun:

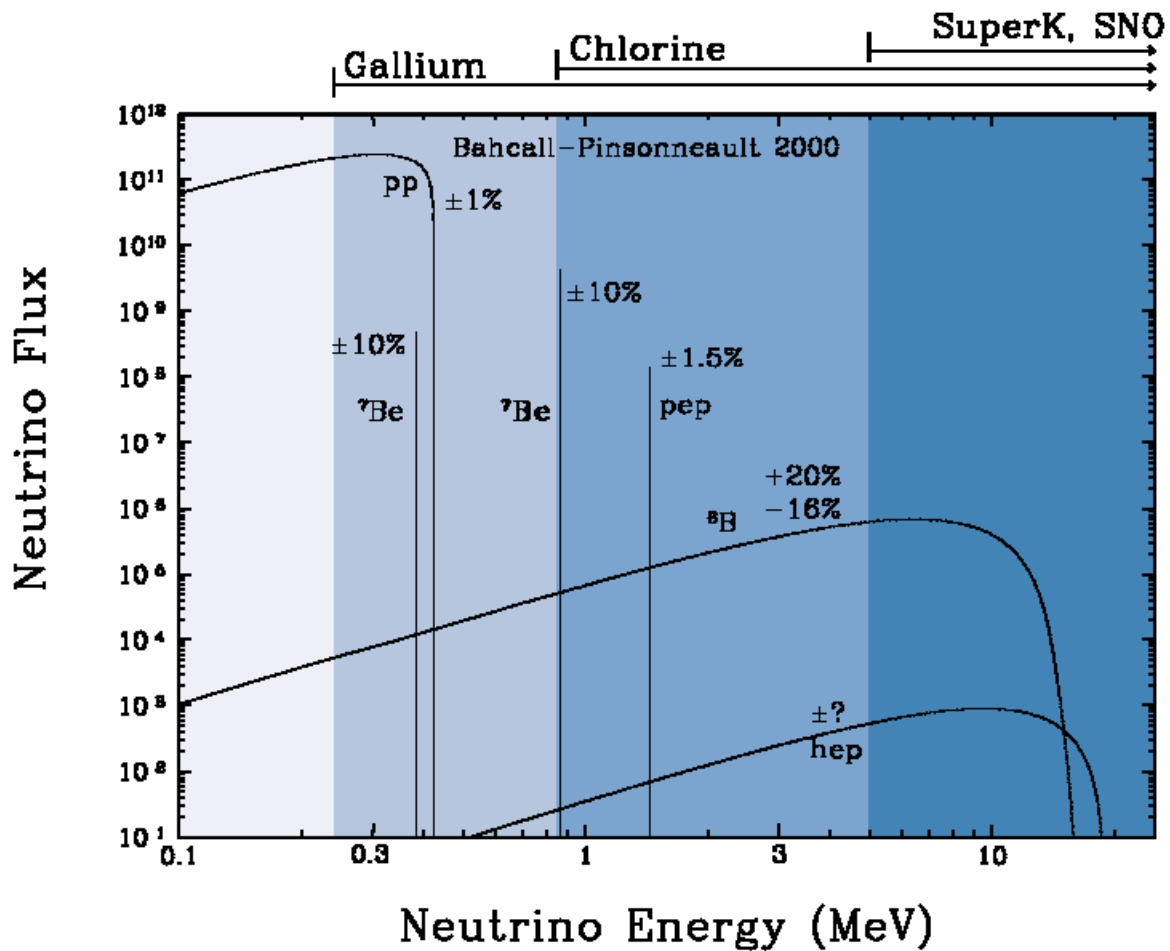
  - the luminosity has increased by 40%.

  - the core temperature has increased by 16%.

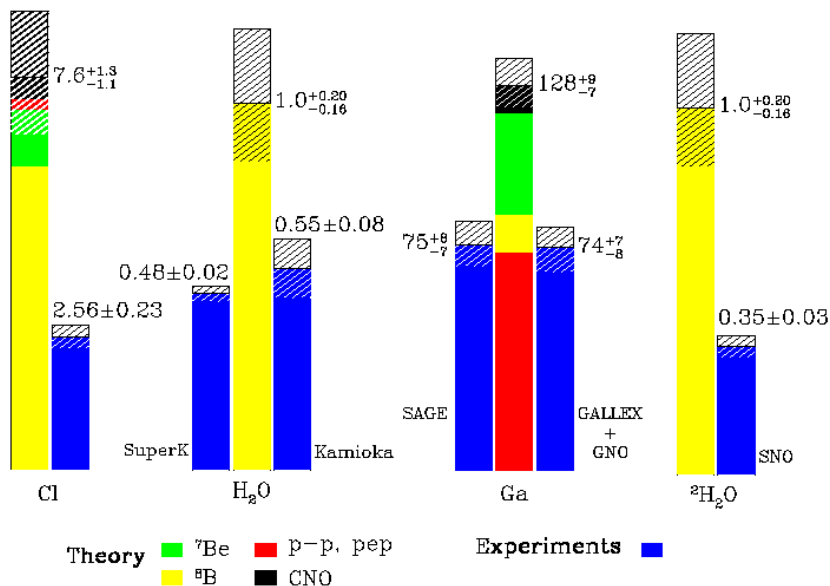
  - the flux of 8B neutrinos has increased by a factor of 40.

# Solar p-p chain



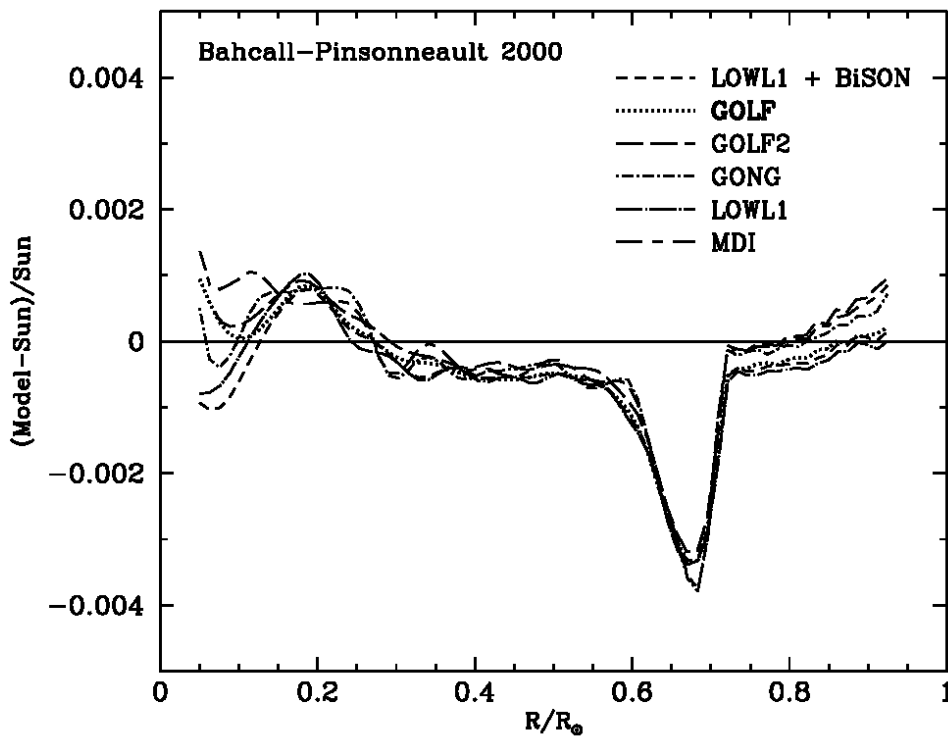
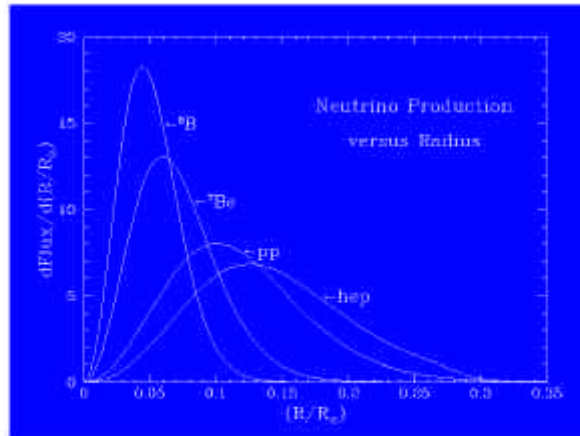


Total Rates: Standard Model vs. Experiment  
Bahcall-Pinsonneault 2000



# Sound speed in Sun from helioseismology

Bahcall



$$\frac{d c}{c} \cong \frac{1}{2} \left( \frac{d T}{T} - \frac{d m}{m} \right) \quad R(^7\text{Be} + p) \propto T^{24}$$

$$\left| \frac{d c}{c} \right| \leq 0.001 \Rightarrow \left| \frac{d T}{T} \right| \leq 0.002$$

$$R(^7\text{Be} + p) \propto T^{24} \Rightarrow \left| \frac{d R}{R} \right| \leq 0.05$$

Source	Flux ( $10^{10} \text{ cm}^{-2}\text{s}^{-1}$ )	Cl (SNU)	Ga (SNU)
pp	$5.95 \times 10^0 \left(1.00^{+0.01}_{-0.01}\right)$	0.00	69.7
pep	$1.40 \times 10^{-2} \left(1.00^{+0.01}_{-0.01}\right)$	0.22	2.8
hep	$9.3 \times 10^{-7}$	0.04	0.1
${}^7\text{Be}$	$4.77 \times 10^{-1} \left(1.00^{+0.09}_{-0.09}\right)$	1.15	34.2
${}^8\text{B}$	$5.93 \times 10^{-4} \left(1.00^{+0.14}_{-0.15}\right)$	6.76	14.2
${}^{13}\text{N}$	$5.48 \times 10^{-2} \left(1.00^{+0.19}_{-0.13}\right)$	0.09	3.4
${}^{15}\text{O}$	$4.80 \times 10^{-2} \left(1.00^{+0.22}_{-0.15}\right)$	0.33	5.5
${}^{17}\text{F}$	$5.63 \times 10^{-4} \left(1.00^{+0.12}_{-0.11}\right)$	0.00	0.1
Total		$8.59^{+1.1}_{-1.2}$	$130^{+9}_{-7}$

Table 1: Standard Model Predictions (BP00 + New  ${}^8\text{B}$ ): solar neutrino fluxes and neutrino capture rates, with  $1\sigma$  uncertainties from all sources (combined quadratically). The neutrino fluxes are the same as in the original BP00 model [12] except for the  ${}^8\text{B}$  flux, which is increased because of the larger adopted value of  $S_{17}(0)$ , see eq. (2.1). Using the 1998 standard value  $S_{17}(0) = 19^{+4}_{-2} \text{eVb}$  [19], the  ${}^8\text{B}$  neutrino flux was calculated previously to be  $\phi({}^8\text{B}) = 5.05 \left(1.00^{+0.20}_{-0.16}\right)$ . The total rates were calculated using the neutrino absorption cross sections and their uncertainties that are given in ref. [20]

<Fractional uncertainty>	pp	${}^3\text{He}{}^3\text{He}$	${}^3\text{He}{}^4\text{He}$	${}^7\text{Be} + p$	$Z/X$	opac	lum	age	diffuse	Total
	0.017	0.060	0.094	0.040	0.061		0.004	0.004	0.15	
<b>Flux</b>										
pp	0.002	0.002	0.005	0.000	0.004	0.003	0.003	0.0	0.003	0.009
${}^7\text{Be}$	0.016	0.023	0.080	0.000	0.034	0.028	0.014	0.003	0.018	0.098
${}^8\text{B}$	0.040	0.021	0.075	0.040 (0.105)	0.079	0.052	0.028	0.006	0.040	0.144 (0.175)
<b>SNU<sub>s</sub></b>										
Cl	0.3	0.2	0.6	0.3	0.6	0.4	0.2	0.04	0.3	
Ga	1.3	1.0	3.3	0.6	3.1	1.8	1.3	0.20	1.5	

${}^7\text{Be}(p,\gamma){}^8\text{B}$  astrophysical S-factor  
from precision cross section measurements\*

A.R. Junghans, E.C. Mohrmann,  
K.A. Snover, T.D. Steiger, E.G. Adelberger,  
J.M. Casandjian, H.E. Swanson

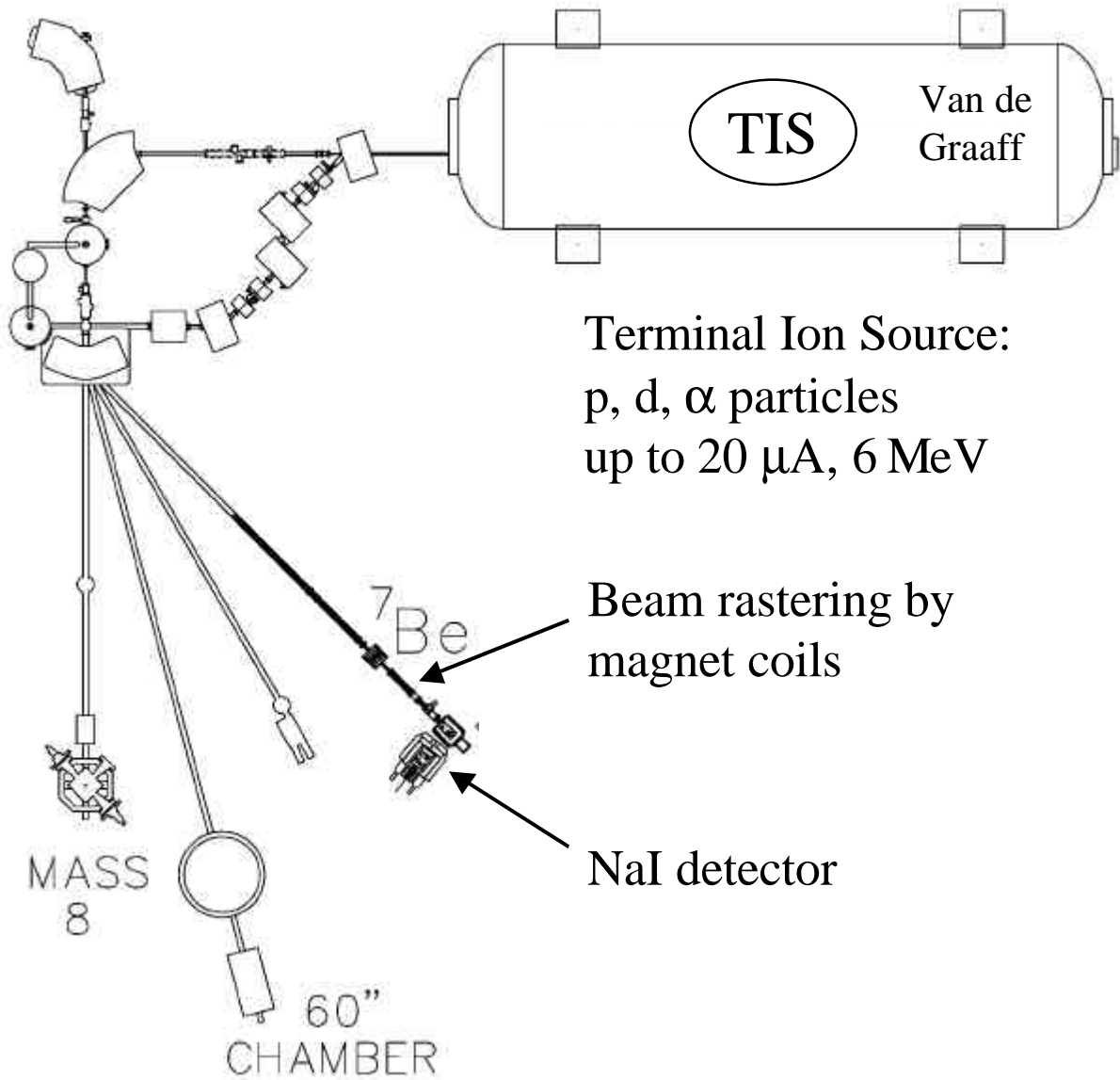
Center for Experimental Nuclear Physics and Astrophysics  
University of Washington, Seattle

L.R. Buchmann, A. Laird, S. Park, A.Y. Zyuzin  
TRIUMF, Vancouver B.C.

\*Phys. Rev. Lett. 88, 041101 (2002). 28-Jan-2002

Supported by the U.S. D.o.E. Grant DE-FG03-97ER41020  
and the N.S.E.R.C. of Canada

# Experimental Setup at U of Washington



Terminal Ion Source:  
p, d,  $\alpha$  particles  
up to 20  $\mu\text{A}$ , 6 MeV

Beam rastering by  
magnet coils

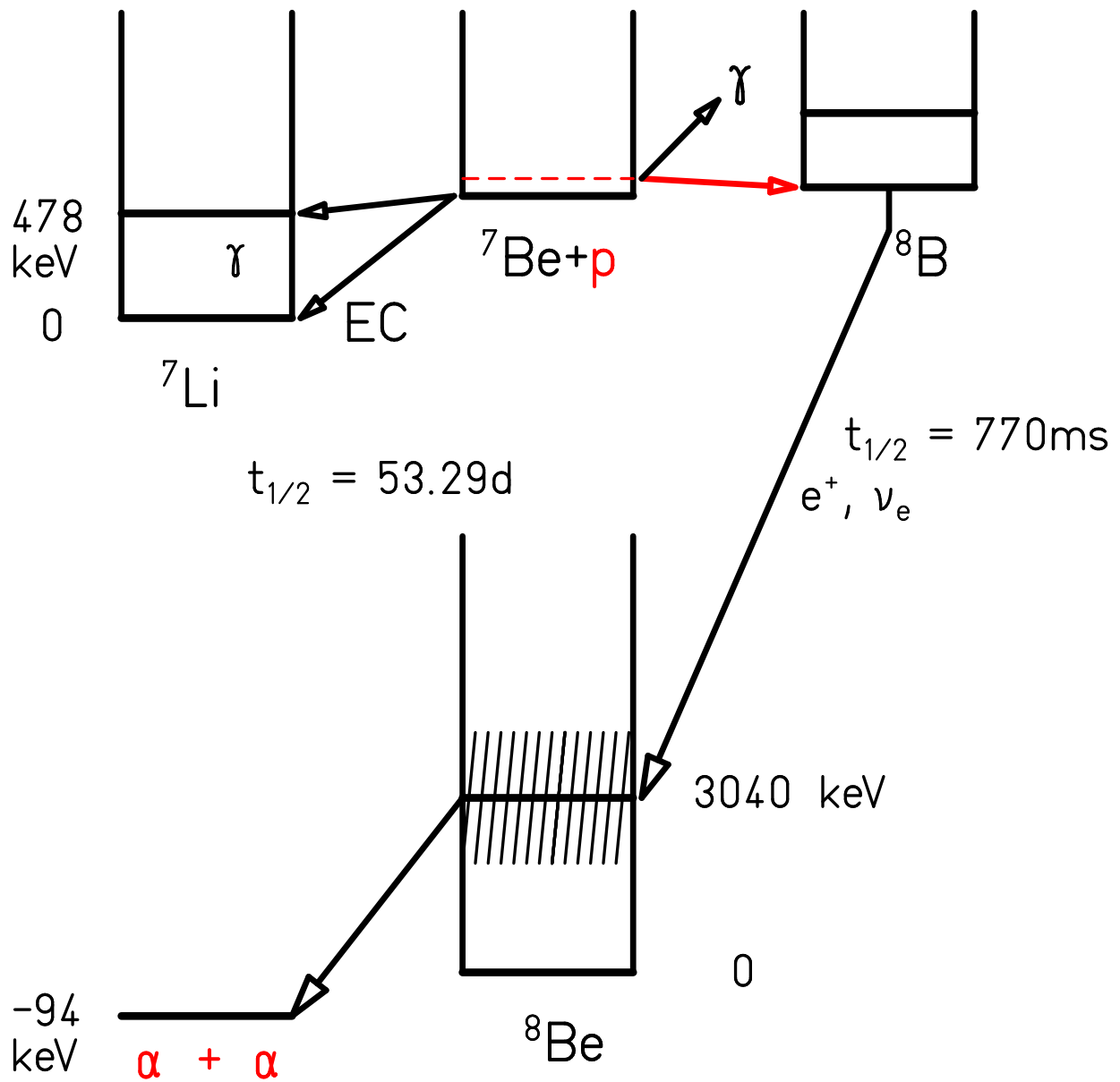
NaI detector

MASS  
8

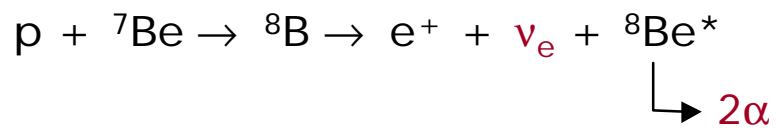
60"  
CHAMBER

# Energy scheme:

- ${}^7\text{Be}$  EC decay
- Radiative proton capture



## Measurement of $p + {}^7\text{Be}$ fusion



Chamber view



## Principle of the measurement:

$$Y = s \cdot \int \frac{dN}{dA} \cdot \frac{dI}{dA} \cdot dA$$

$$= s \cdot \frac{dN}{dA} \cdot I \quad \text{true when target areal density } \frac{dN}{dA} = \text{constant}$$

large area target, small area beam (conventional technique)

$$= s \cdot N \cdot \frac{dI}{dA} \quad \text{true when beam flux } \frac{dI}{dA} = \text{constant}$$

small area target, large area beam (present technique)

If the areal density of **target** (**beam**) is not constant, then one must know also the areal density of the **beam**(**target**).

Cross section:

$$s(\bar{E}_{c.m.}) = \frac{Y_a(E_p) \cdot F_a(E_p) \cdot \beta(^8B)}{2 \cdot N_p \cdot N_{Be}(t) \cdot \Omega / 4\pi}$$

$E_p$  = bombarding energy

$Y_\alpha(E_p)$  =  $\alpha$  yield above 895 keV threshold energy

$F_\alpha(E_p)$  = correction for  $\alpha$  yield below threshold

$N_p$  = integrated number of protons per cm<sup>2</sup>

$N_{Be}(t)$  = # of <sup>7</sup>Be atoms at time of measurement

$\Omega$  = solid angle of the  $\alpha$  detector

$\bar{E}_{c.m.}$  = mean c.m. energy averaged over target

$\beta(^8B)$  = rotation timing efficiency

## Timing factor $\beta(^8\text{B})$

$$\mathbf{b}(^8\text{B}) = \frac{I t_1 \left[ 1 - e^{-I(t_1+t_2+t_3+t_4)} \right]}{(1 - e^{-I t_1}) \left[ e^{-I t_2} - e^{-I(t_1+t_2)} \right]}$$

$\lambda$  = decay rate of  $^8\text{B}$ ;  $t_{1/2} = 770 \pm 3$  ms

$t_1$  = bombardment time

$t_2$  = transfer time to counting

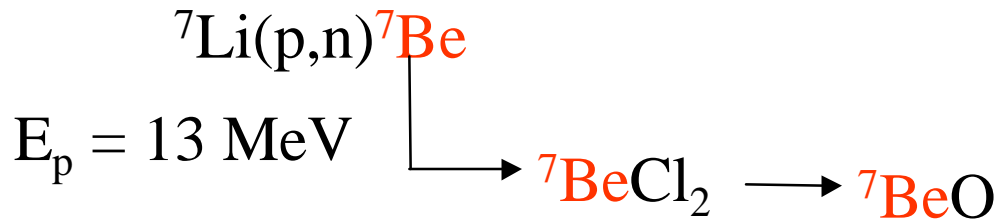
$t_3$  = counting time

$t_4$  = transfer time to bombardment

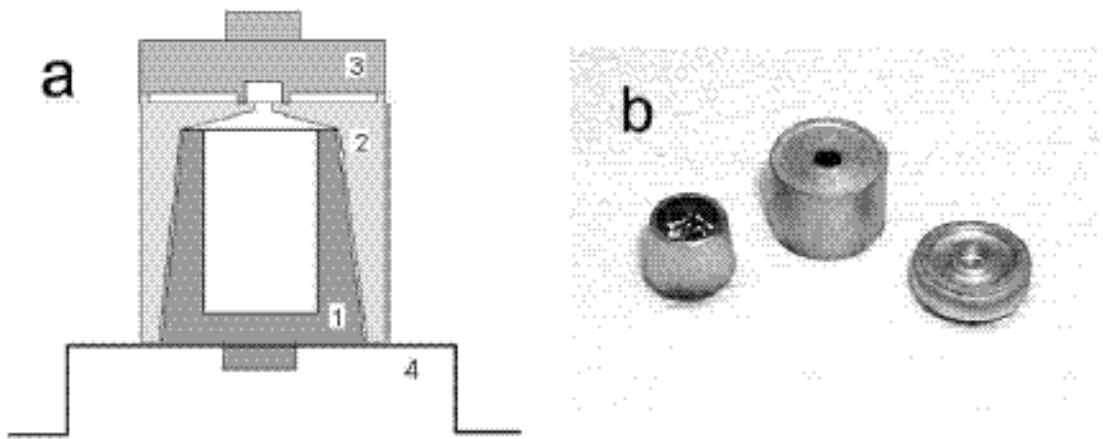
$\beta(^8\text{B})^{-1}$  = inverse of timing efficiency

= fraction of  $^8\text{B}$  decays which take place in front of detector

# $^7\text{Be}$ target fabrication (TRIUMF)

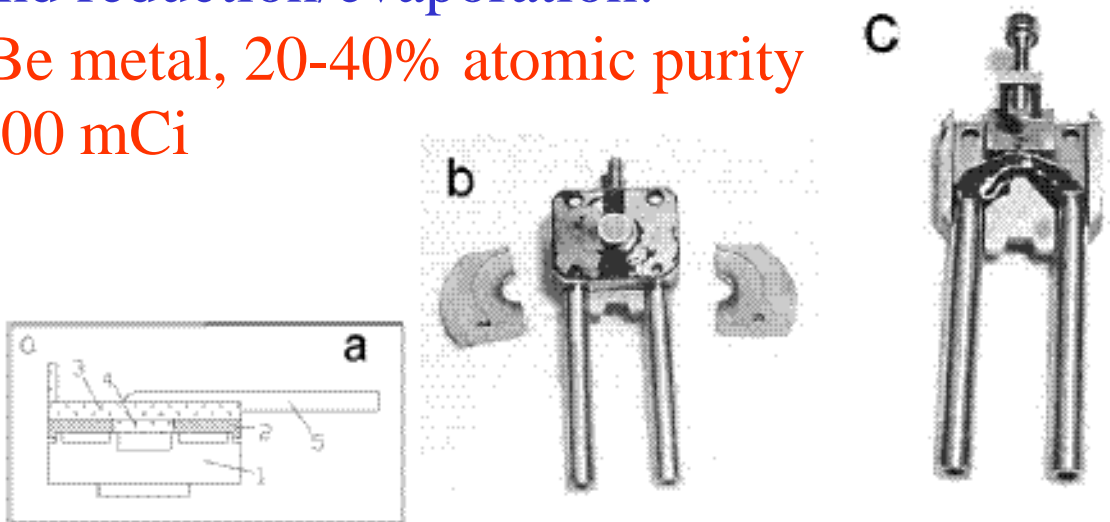


First reduction/evaporation:



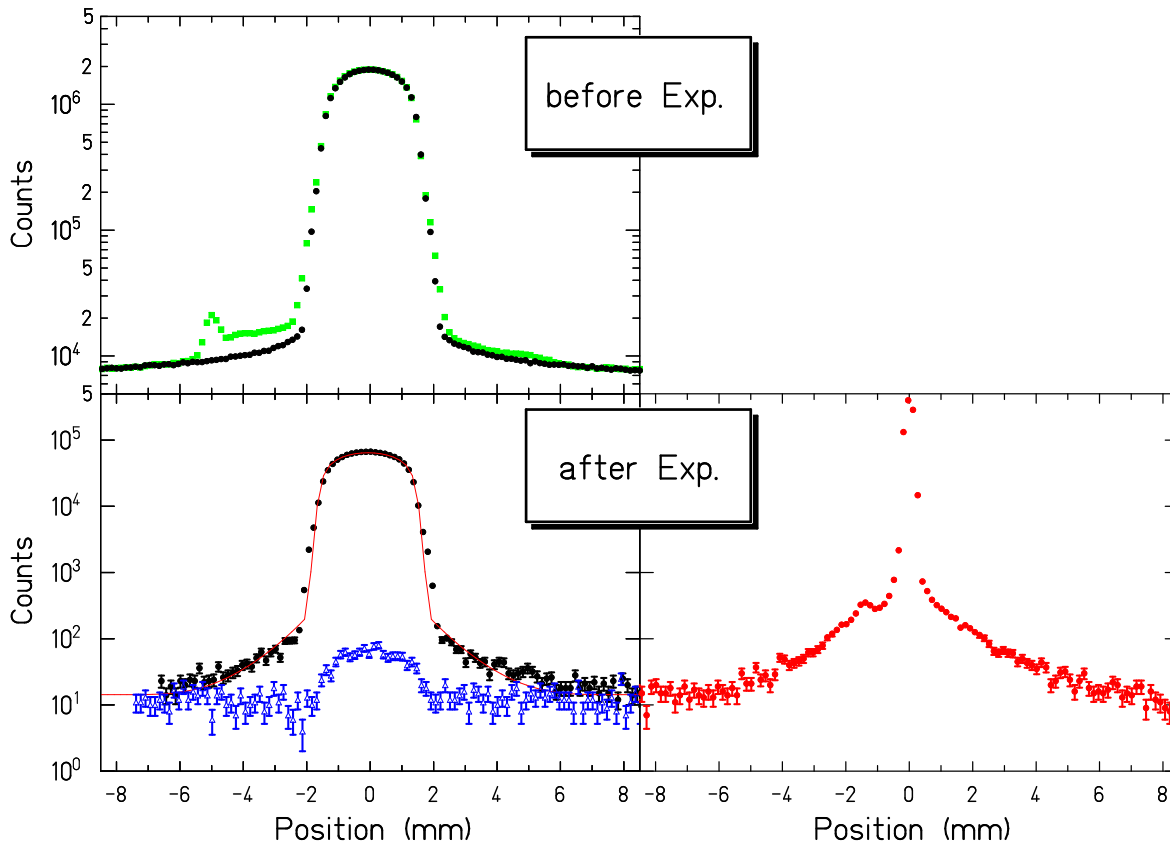
Second reduction/evaporation:

$\Rightarrow$   $^7\text{Be}$  metal, 20-40% atomic purity  
100 mCi



4mm dia. post backing  
(Mo)

## Scans of Target Density Distribution:



Horizontal line scan of target activity:

→ Target density integrated over one dimension

Washer breakoff removes the activity tail

Fit of target density:

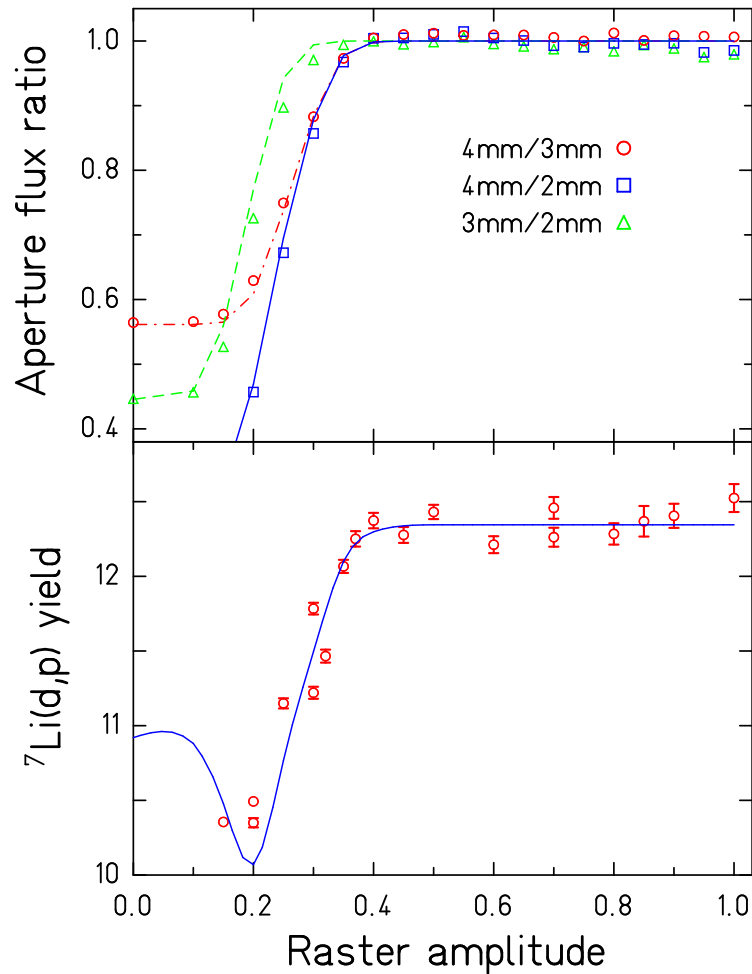
Center distribution diameter 3.1 mm

Tail (27% central density) 3.1 - 3.4 mm

Scan before and after (p,γ) experiment:

→ Target distribution unchanged

## Beam & target uniformity:



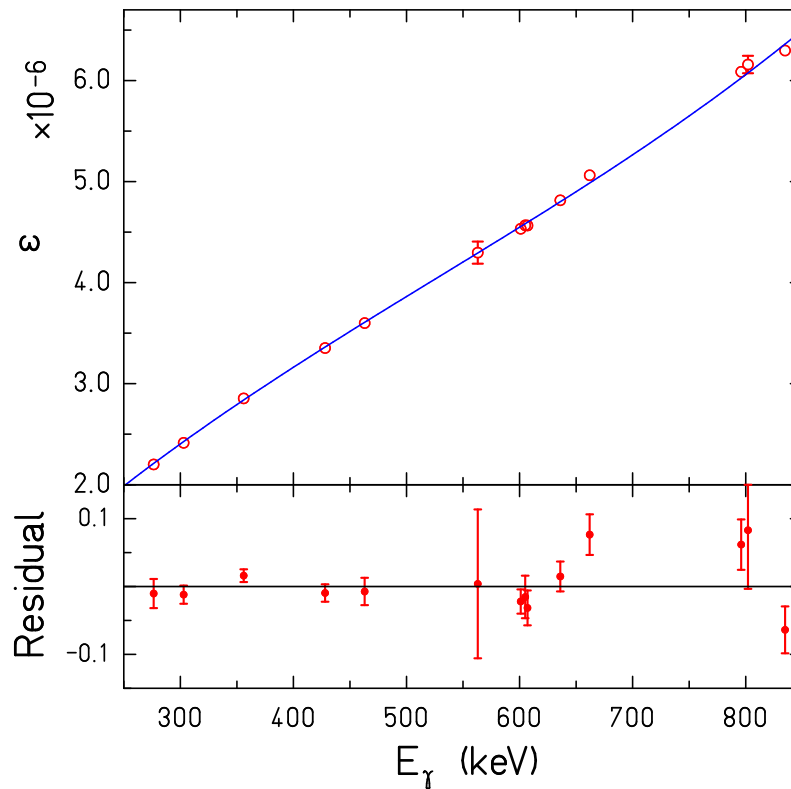
Aperture flux ratio is unity for a homogeneous beam flux

Normalized Yield is constant, when product of beam and target density is uniform.

## Highlights:

- Large area uniform beam flux - small area target  
→ precision determination of beam-target interactions
- ${}^7\text{Be}(\alpha, \gamma){}^{11}\text{C}$  narrow resonance profile  
→ precision determination of target energy loss profile
- In situ monitoring of  ${}^7\text{Be}$  activity  
→ precision determination of Number of  ${}^7\text{Be}$  atoms & sputtering losses
- Clean cryopumped vacuum system & multiple  $\text{LN}_2$  cold traps  
→ no carbon buildup, as evidenced by repeated  ${}^7\text{Be}(\alpha, \gamma)$  measurements
- Direct measurement of  ${}^8\text{B}$  backscattering losses  
→ this potentially important aspect is shown to be small in this work
- Measurement of all important sources of systematic error

## Ge-Calibration



$^{54}\text{Mn}$ ,  $^{125}\text{Sb}$ ,  $^{133}\text{Ba}$ ,  $^{134}\text{Cs}$ ,  $^{137}\text{Cs}$  sources (0.8%,  $1\sigma$ )

Fit  $\chi^2/\nu = 2.2$

Relative activity with an independently calibrated  $^{137}\text{Cs}$  source (0.4%,  $1\sigma$ ) agrees to  $\pm 0.1\%$

Calibration in situ

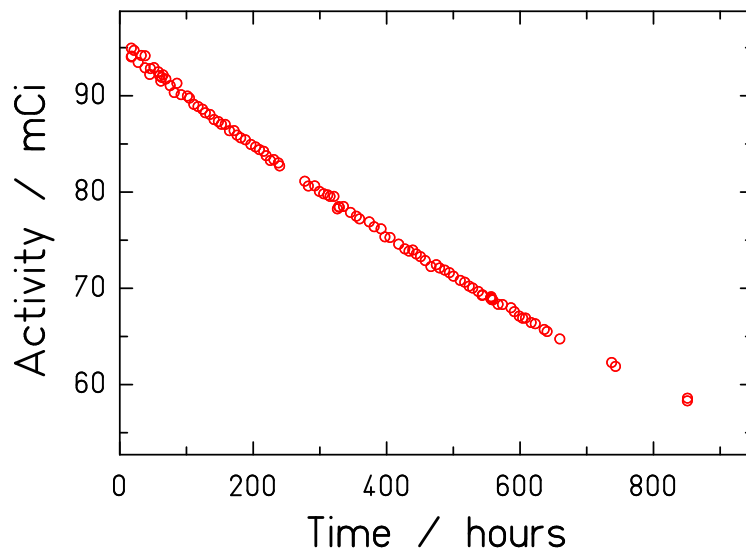
$$\epsilon(478 \text{ keV}) = 3.77 \pm 0.05 \cdot 10^{-6}$$

Absolute Activity of the  $^7\text{Be}$  target:

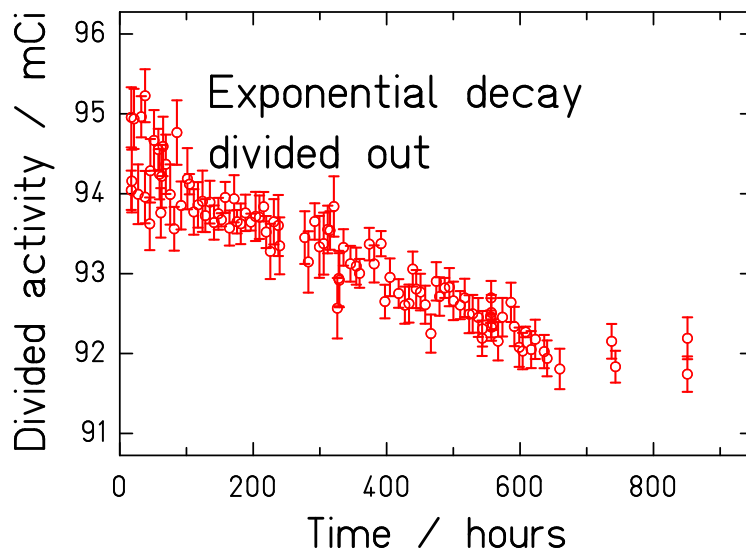
$$A(^7\text{Be}) = \frac{N_\gamma}{\Delta t F_{\text{lt}} \epsilon \text{ BR}} \quad \text{BR} = 10.52 \pm 0.06\%$$

Overall systematic uncertainty: 1.9%

## Absolute Target activity

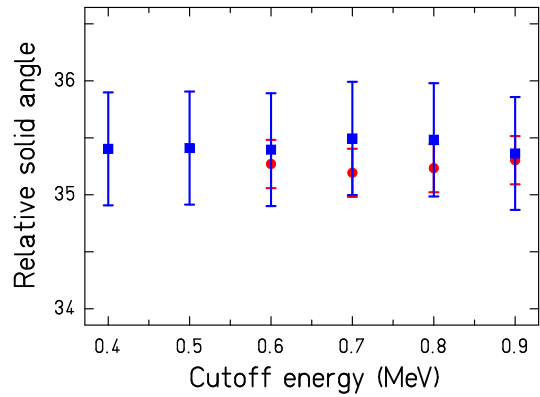
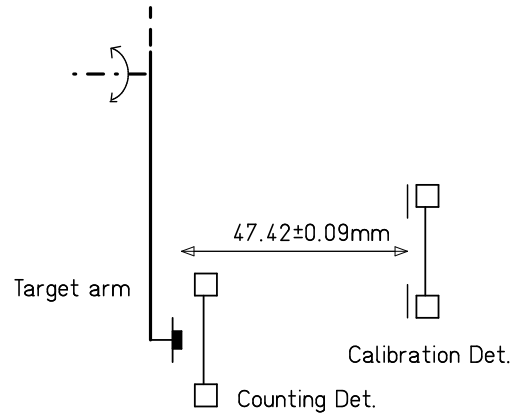
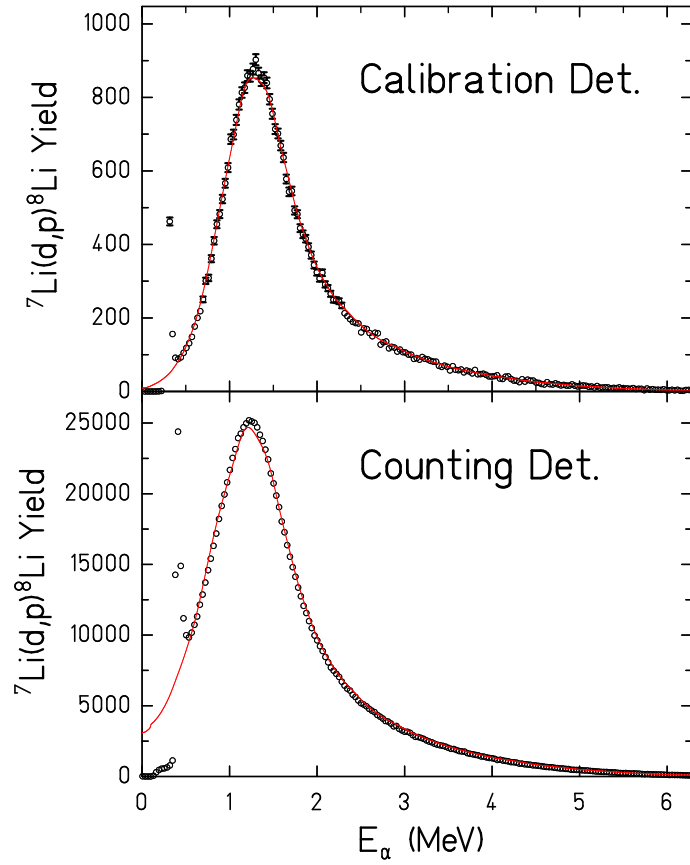


Collimated Ge detector to monitor  ${}^7\text{Be}$  activity, calibrated in the experimental geometry.



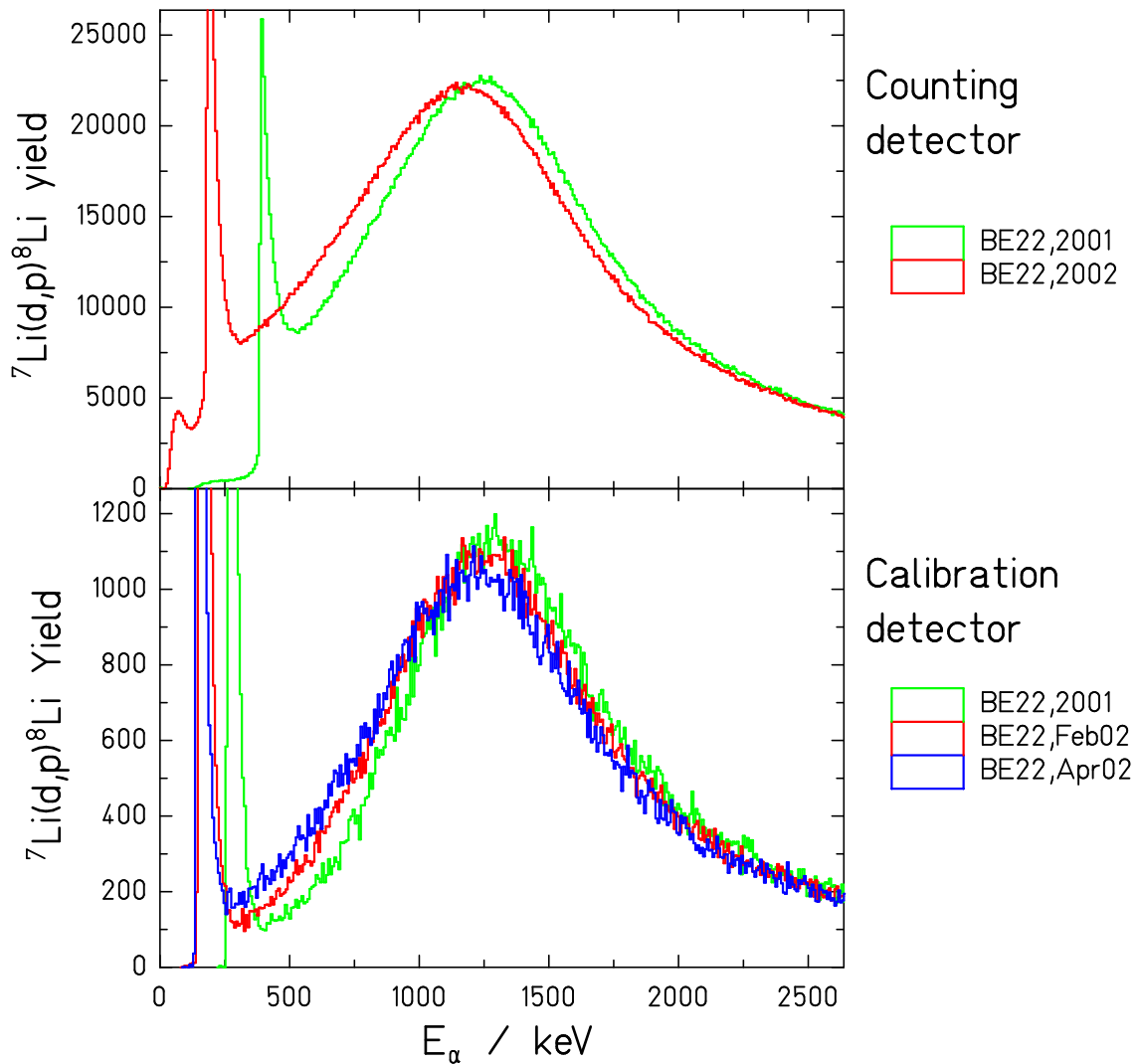
→ Small losses due to sputtering.  
Absolute activity determined to 2%.

# Solid Angle Determination:



${}^7\text{Li}(d,p){}^8\text{Li}$  Yield from  ${}^7\text{Be}$  and  $\text{LiF}$  targets

## $^7\text{Li}$ diffusion into the backing

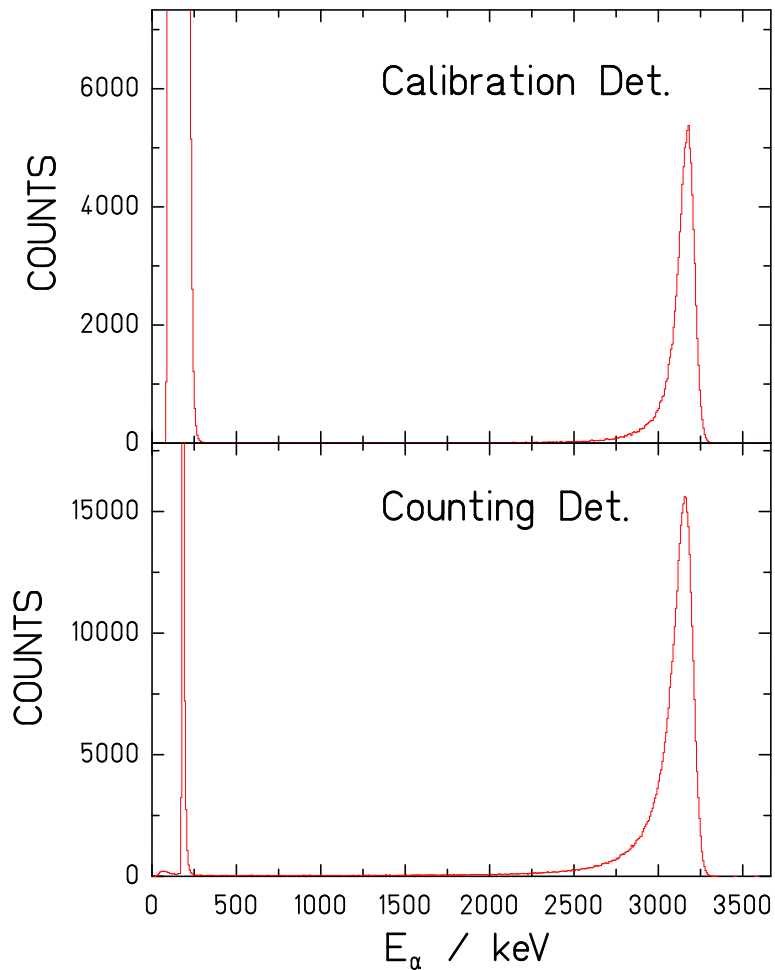


$^7\text{Li}(d,p)^8\text{Li}$  was used for relative solid angle determination  
 $^7\text{Li}$  diffuses into the Mo backing and causes higher  $\Delta E$  of  $\alpha$ 's

Correction for spectral cut-off is not reliable.

Solid angle determination based on (d,p) yields is incorrect.

## Solid Angle from $^{148}\text{Gd}$ source measurement



$^{148}\text{Gd}$  source on a Mo-backing

Absolute solid angle of calibration detector  
given by collimator-target geometry

$$\Omega_{\text{cal}} = 0.1092 \pm 0.0004 \text{ sr}$$

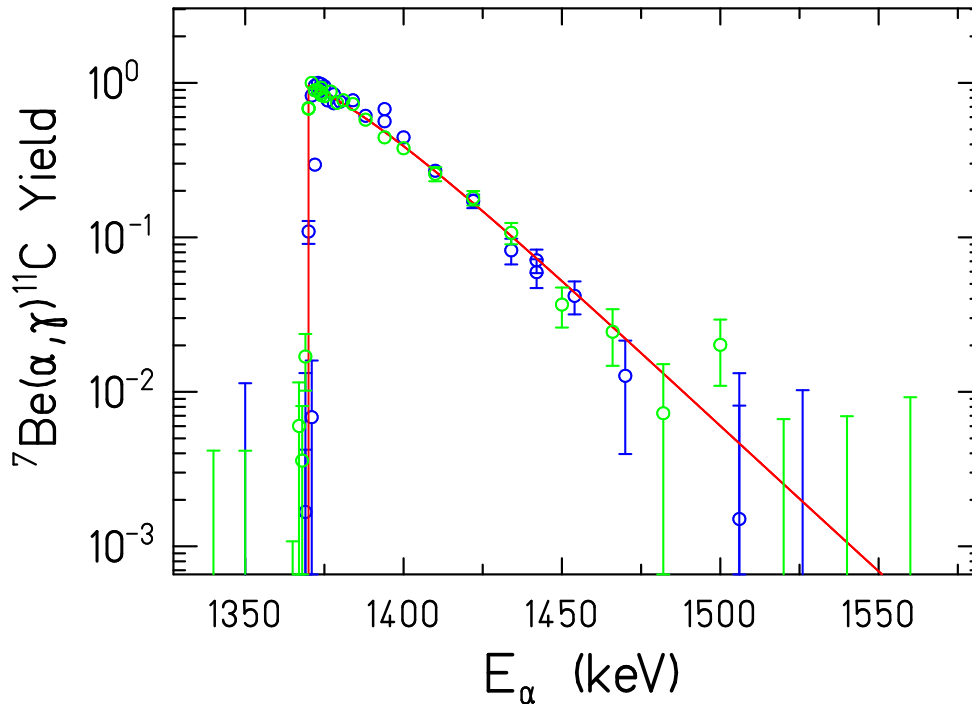
Relative solid angle of counting-detector to  
calibration detector given from ratio of count rates

$$\frac{\Omega_{\text{cal}}}{\Omega_{\text{cou}}} = 39.57 \pm 0.39$$

→ Absolute solid angle of counting detector

$$\Omega_{\text{cou}} = 4.32 \pm 0.04 \text{ sr}$$

## Target width



Sharp Resonance in  ${}^7\text{Be}(\alpha, \gamma){}^{11}\text{C}$  at  $E_\alpha = 1.376$  MeV

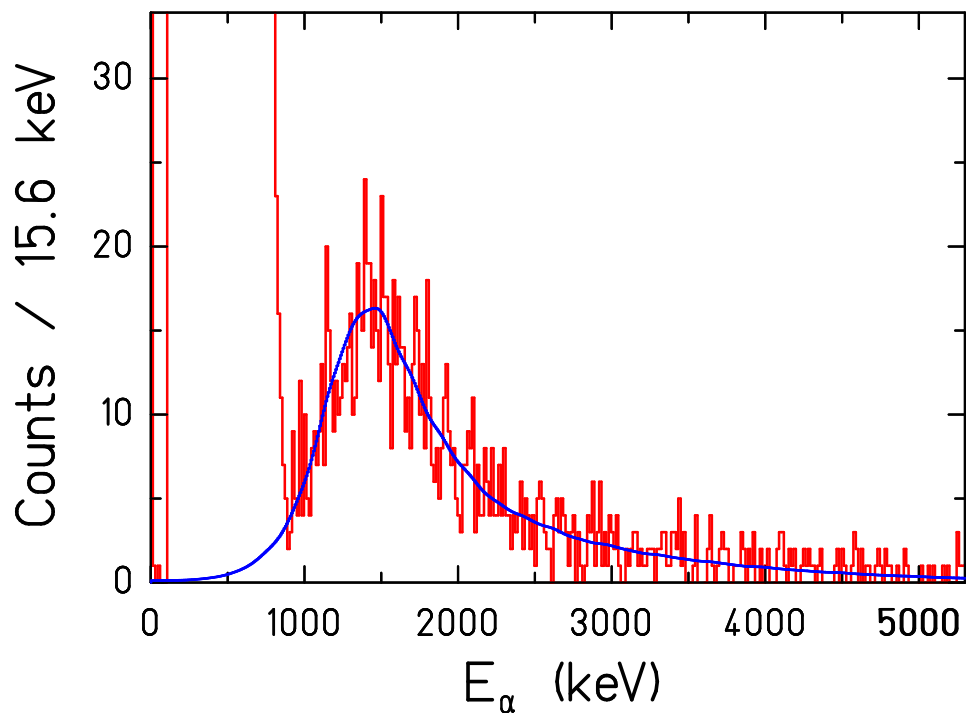
Excellent reproducibility of apparent resonance energy in the middle and after the experiment:  
 $\Delta E_\alpha = 1 \pm 3$  keV, negligible Carbon build-up

Mean energy loss in the target:

$26 \pm 2$ keV	1376 keV	$\alpha$
$9.1 \pm 0.7$ keV	221 keV	p

Atomic  ${}^7\text{Be}$  purity: 20-40%

## ${}^7\text{Be}(p,\gamma){}^8\text{B}$ Spectrum of $\alpha$ particles:



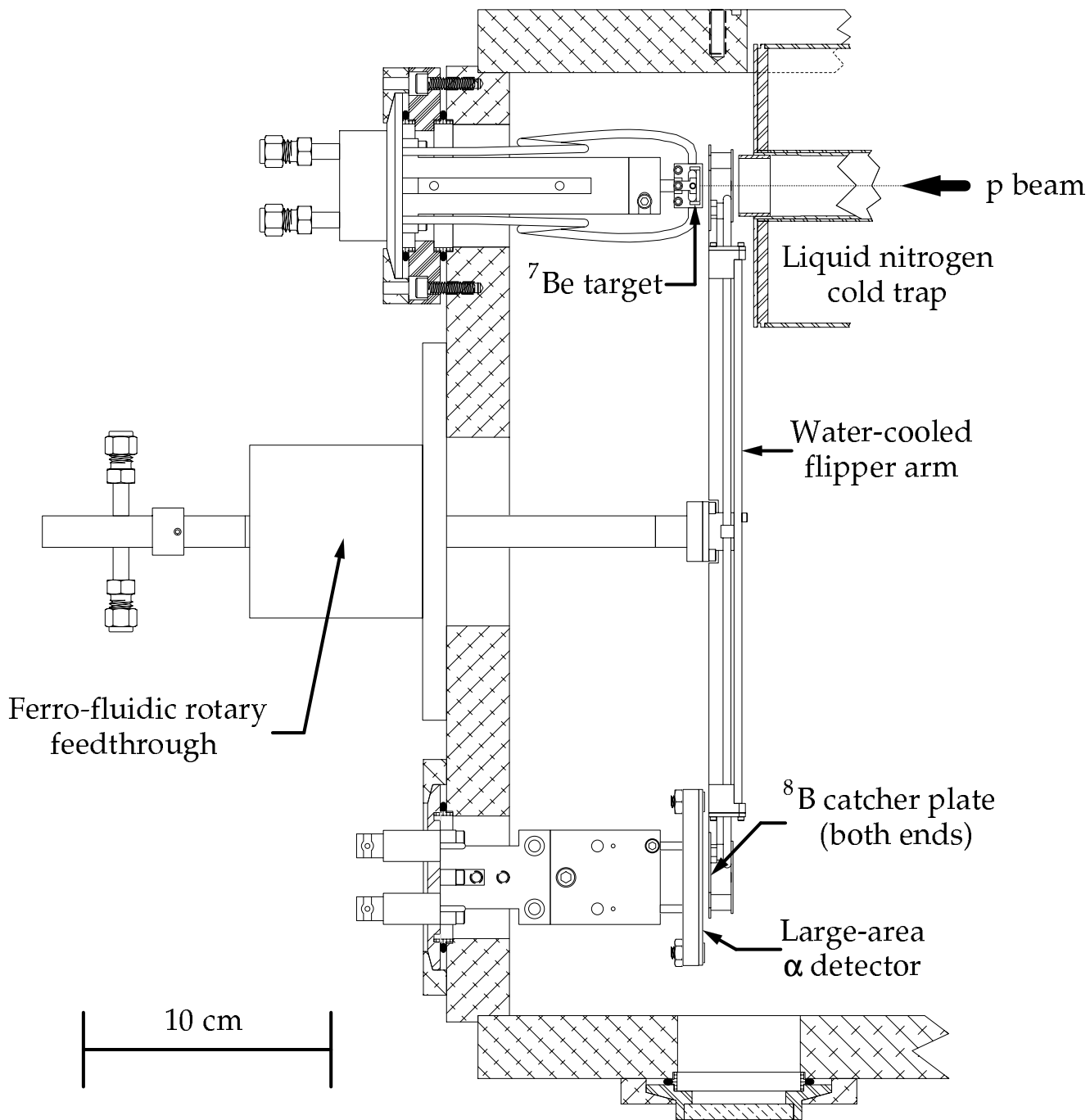
$$E_{\text{cm}}^{\text{av}} = 186 \text{ keV}$$

41 h counting time, event rate 0.5 /min

Noise caused by High  $\gamma$ -flux from  ${}^7\text{Be}$  target

Noise threshold: 895 keV

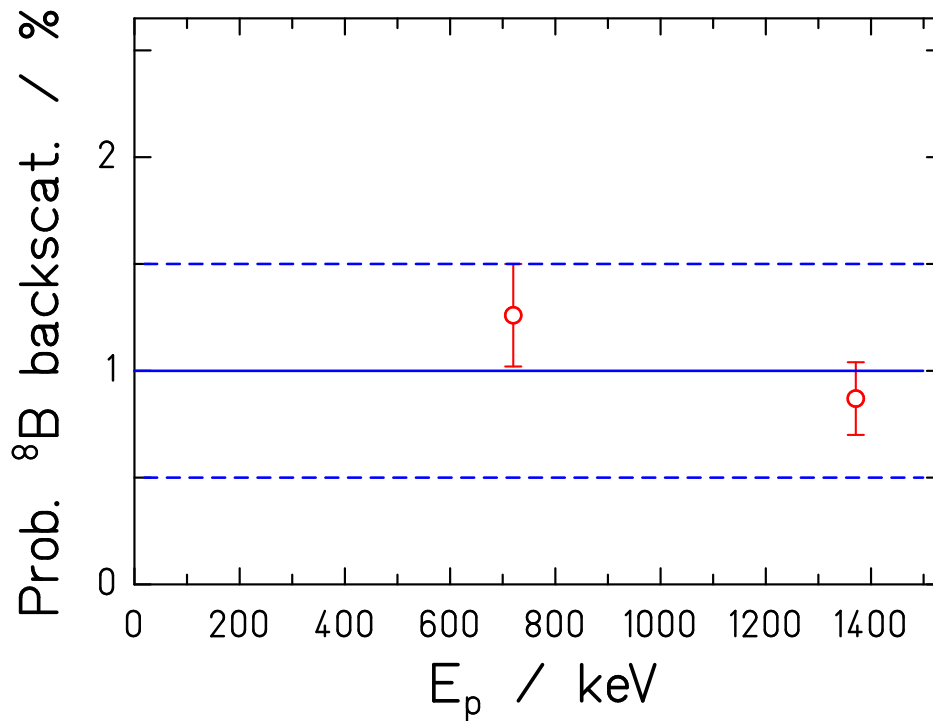
MC Simulated spectrum to compute  
loss due to cutoff: 3.9%



$^8\text{B}$  Backscatter Apparatus

## $^8\text{B}$ backscattering:

First Experiment to measure this effect.

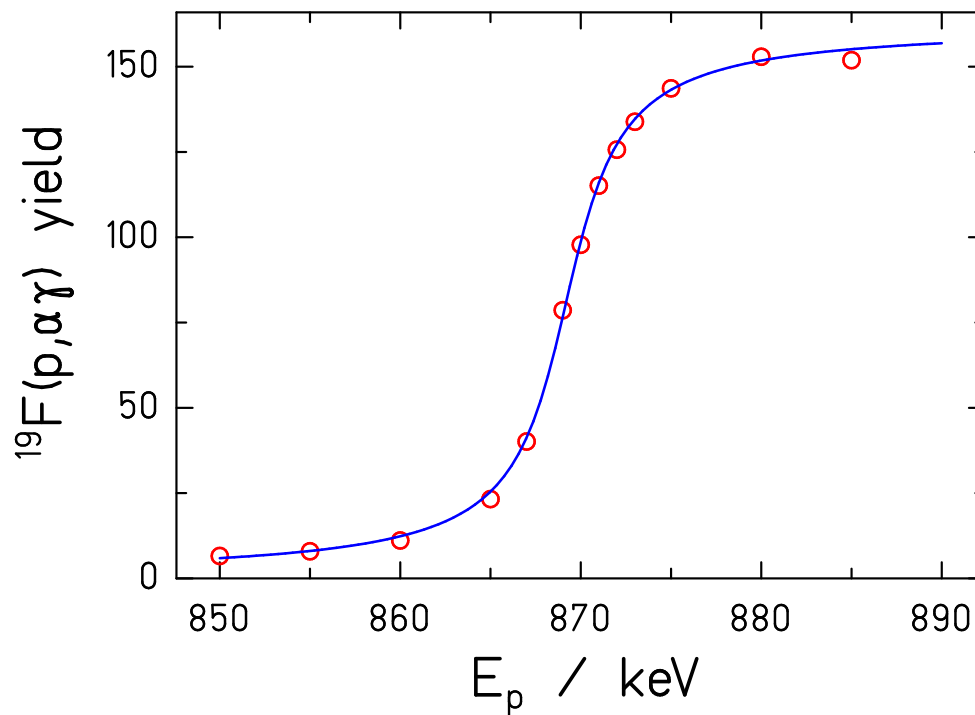


Backscattering probability measured  
for  $E_p = 724$  keV and  $1379$  keV  
→ Correction of  $Y_\alpha$  by  $1 \pm 0.5\%$

Backscattering depending on:

Target thickness, Contaminants  
Backing material, Bombarding energy

## Accelerator Energy Calibration:



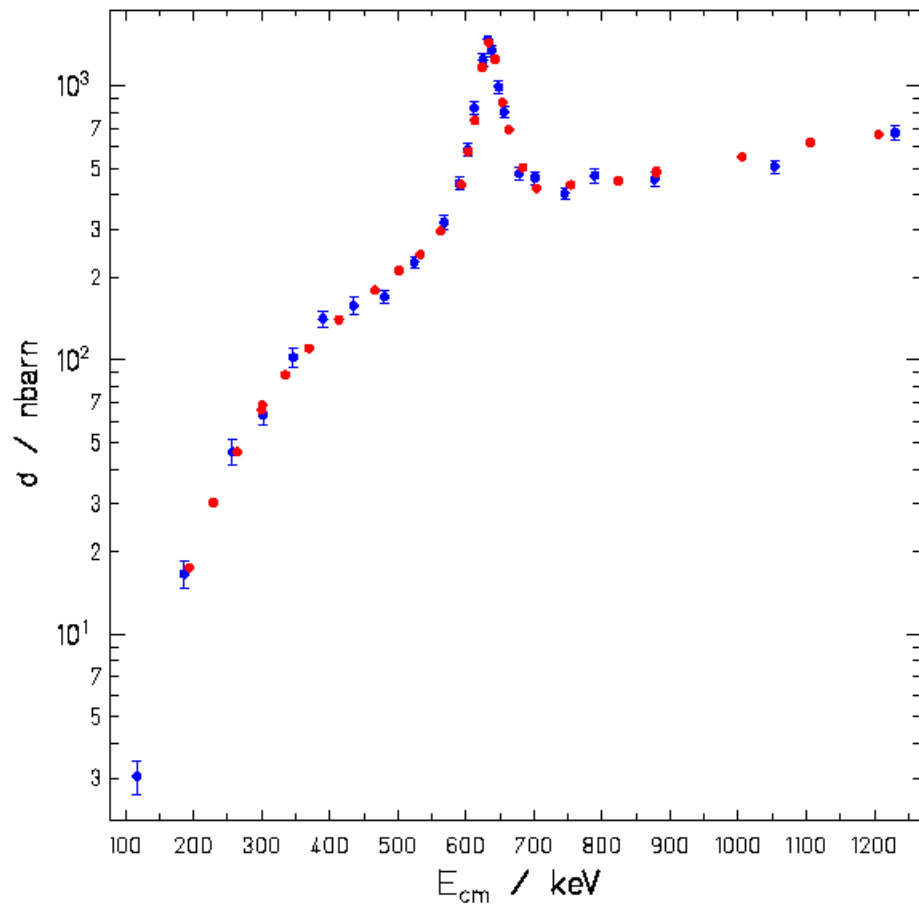
Sharp, well known resonances in  $^{19}\text{F}(p, \alpha \gamma)^{16}\text{O}$   
at  $E_p = 340, 483, 871$  keV

Fit to obtain resonance energy  
Accelerator energy calibration  
to a precision of  $\pm 0.17\%$

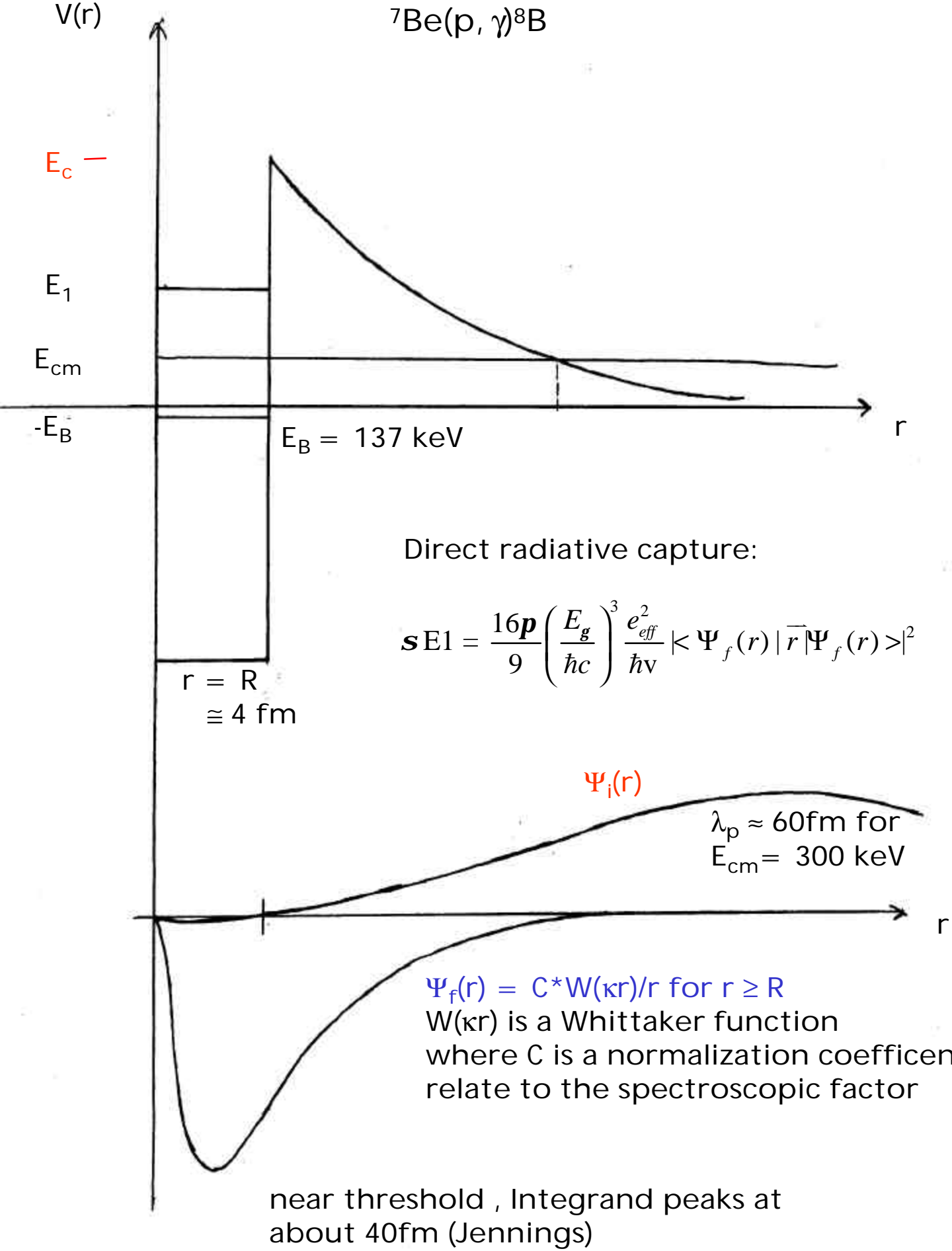
## Error budget:

	Correction	Syst. Err. S(0)
Target activity	-	1.9%
Solid angle	-	2.9%
Beam & target nonuniformity	-	1.0%
Integrated beam flux	-	0.8%
Cutoff in $\alpha$ -spectrum	4-8%	0.7%
Backscattering of $^8\text{B}$	1.0%	0.5%
Beam-off background	0-4%	0.2%
Counting cycle	-	0.2%
Systematic error:		3.7%
Beam energy uncertainty	-	0.2-0.6%
Target composition	-	0-1.1%
Target thickness	-	0-1.0%
Varying systematic error:		0.1-1.5%
Counting statistics per point:		1.0-2.8%

Total error per point:	< 5%
------------------------	------



${}^7\text{Be}(p, \gamma){}^8\text{B}$



## S-factor

$$S(E_{cm}) = \mathbf{s}(E_{cm}) E_{cm} \exp(E_G^{1/2} / E_{cm}^{1/2})$$

$$\text{Gamow energy: } E_G = (2\mu Z_1 Z_2)^2 \mathbf{m} c^2 / 2$$

Purpose: removes the dominant  $E_{cm}$ -dependence of  $\sigma$  due to s-wave Coulomb barrier penetration and deBroglie wavelength in entrance channel.

Derivation: represent a slowly varying "direct" cross section as the tail of a distant resonance:

$$a + A \rightarrow b + B$$

$$\Rightarrow \mathbf{s}(E_{cm}) = \mathbf{p} \hat{\lambda}_a^2 \mathbf{w} \frac{\Gamma_a \Gamma_b}{(E - E_R)^2 + \Gamma^2 / 4} \quad \mathbf{w} = \frac{(2J+1)}{(2s+1)(2I+1)}$$

for  $E_{cm} \square E_R$ , denominator is slowly varying,  $\Rightarrow$

$$\Rightarrow \mathbf{s}(E_{cm}) \propto \hat{\lambda}_a^2 \Gamma_a \Gamma_b$$

where  $\Gamma_a$  = formation width of resonance "state"

$\Gamma_b$  = decay width of resonance "state"

$$\hat{\lambda}_a^2 = \left[ \frac{\hbar}{\mathbf{m}v} \right]^2 = \frac{\hbar^2}{2\mathbf{m}E_{cm}}$$

$v$  = relative velocity of  $a+A$  (at infinity)

$$\mathbf{m} = M_a M_A / (M_a + M_A) \quad \text{and} \quad E_{cm} = M_A E_{lab} / (M_a + M_A)$$

$$\Rightarrow \text{Now } \Gamma_a = \frac{3\hbar v}{R} P_\ell \mathbf{q}_\ell^2$$

where  $R \cong R_a + R_A \cong 1.4(A_a^{1/3} + A_A^{1/3})$  (fm)

$\mathbf{q}_\ell^2$  = reduced width of the resonant "state"

$P_\ell$  = the Coulomb penetrability for  $a+A$

for orbital angular momentum  $\ell$

Now in WKB approximation

$$\Rightarrow P_\ell = \frac{|\mathbf{c}_a(R)|^2}{|\mathbf{c}_a(\infty)|^2} \cong (E_c/E_{cm})^{1/2} \exp \left[ -\frac{2\sqrt{2}\mathbf{m}}{\hbar} \int_R^{R_0} \left( \frac{E_c R}{r} + \frac{E_\ell R^2}{r^2} - E_{cm} \right) dr \right]$$

$$\text{where } E_c = \frac{Z_1 Z_2 e^2}{R} \cong \frac{Z_1 Z_2}{R(\text{fm})} (\text{MeV}) = \text{Coulomb barrier energy}$$

$$R_0 = Z_1 Z_2 e^2 / E_{cm} = \text{classical turning point}$$

$$E_\ell = \frac{\ell(\ell+1)\hbar^2}{2\mathbf{m}R^2} = \text{centrifugal barrier energy} = 0 \text{ for s-wave}$$

$$\Rightarrow \text{Hence } \Gamma_a \propto v \cdot P_\ell \propto \exp[-W] \text{ where } -W \text{ is the exponential part of } P_\ell$$

Doing the integral and expanding the result in powers of  $E/E_c$

$$\Rightarrow \text{yields } W = \frac{E_G^{1/2}}{E_{cm}^{1/2}} \left[ 1 - \frac{4}{\mathbf{p}} \left( \frac{E_{cm}}{E_c} \right)^{1/2} + \frac{2}{3\mathbf{p}} \left( \frac{E_{cm}}{E_c} \right)^{3/2} \right]$$

note the second term in the above expansion is

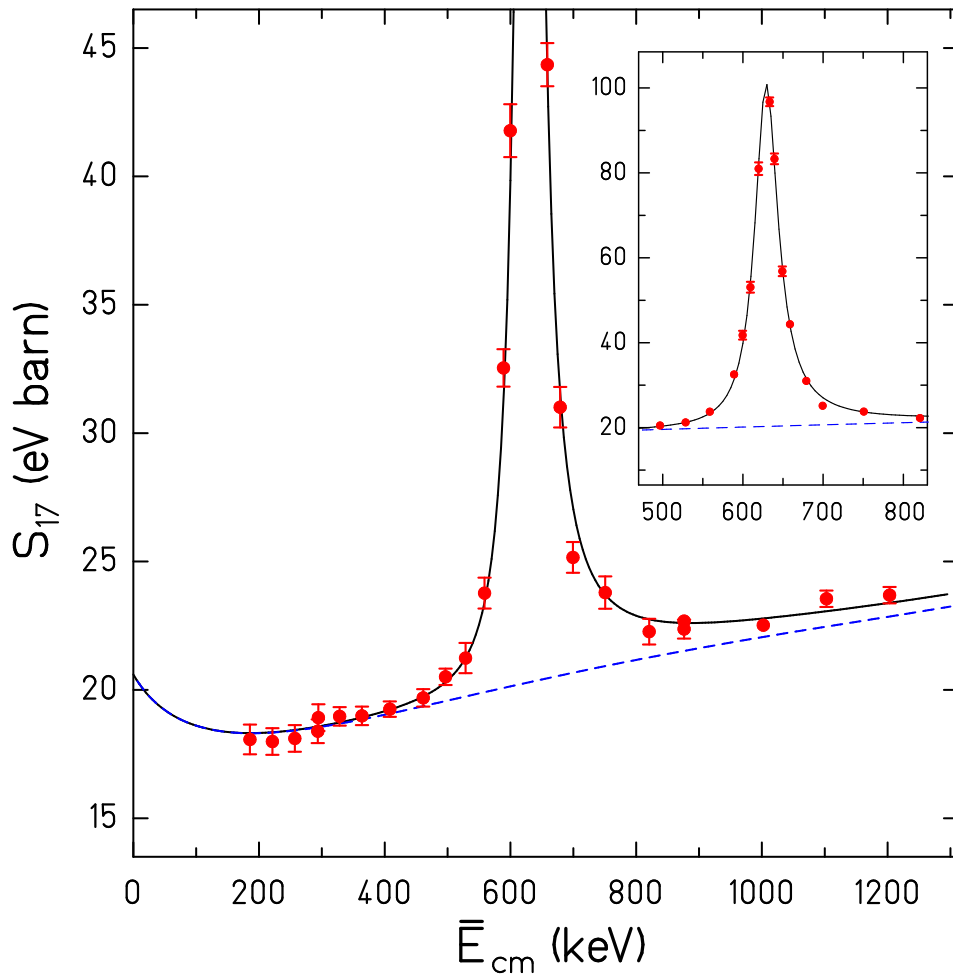
$$\Rightarrow -\frac{E_G^{1/2}}{E_{cm}^{1/2}} \frac{4}{\mathbf{p}} \left( \frac{E_{cm}}{E_c} \right)^{1/2} = -\frac{4}{\mathbf{p}} \left( \frac{E_G}{E_c} \right)^{1/2} = -\frac{4}{\hbar} \sqrt{2Z_1 Z_2 e^2 \mathbf{m} R}$$

which depends on  $R$  but not  $E_{cm}$

Note for  ${}^7\text{Be}+p$ ,  $R \cong 4\text{fm}$ ,  $E_c \cong 1 \text{ MeV}$ ,

direct capture predominantly  $E1 \Rightarrow$  s-wave + d-wave.

## Astrophysical $S_{17}$ factor:



$S_{17}$  fit including resonant capture and [cluster](#) model according to P. Descouvemont & D. Baye, 1994

In  ${}^7\text{Be}(p,\gamma){}^8\text{B}$ , tentatively,

- the rise in  $S(E_{\text{cm}})$  from  $E_{\text{cm}} = 300$  to  $1000$  keV is due to d-wave
- the rise in  $S(E_{\text{cm}})$  below  $E_{\text{cm}} = 300$  keV is due to the capture being increasingly extra-nuclear (i.e. occurs at larger  $R$ ) as  $E_{\text{cm}}$  decreases.

The S-factor does not contain effects due to:

- the finite size of the nucleus
- nuclear structure and strong interaction effects
- antisymmetrization
- contribution from other partial waves
- screening by atomic electrons
- final-state phase space

## Fitting $S_{\text{exp}}(E_{\text{cm}})$ vs. $E_{\text{cm}}$

$$S(E_{\text{cm}}) = \frac{\mathbf{s}(E_{\text{cm}})}{E_{\text{cm}}} \exp(-E_G^{1/2} / E_{\text{cm}}^{1/2})$$

$$\mathbf{s}(E_{\text{cm}}) = \mathbf{s}_{\text{res}}(E_{\text{cm}}) + \mathbf{s}_{\text{non-res}}(E_{\text{cm}})$$

$$\mathbf{s}_{\text{res}}(E_{\text{cm}}) = p \tilde{\lambda}_p^2 W \frac{\Gamma_p \Gamma_g}{(E - E_R)^2 + \Gamma^2 / 4}$$

$$\text{where } \Gamma = \Gamma_p + \Gamma_g \cong \Gamma_p,$$

$$E_g = E_{\text{cm}} + Q = E_{\text{cm}} + 0.137 \text{ MeV},$$

$$\Gamma_p(E_{\text{cm}}) = \Gamma_p(E_R) \left[ E_{\text{cm}}^{1/2} P_\ell(E_{\text{cm}}) / (E_R^{1/2} P_\ell(E_R)) \right],$$

$$\Gamma_g = \Gamma_g(E_{R,g}) \left[ E_g / E_{R,g} \right]^3$$

$$\text{and } \tilde{\lambda}_p^2 = \tilde{\lambda}_p^2(E_R) \left[ \frac{E_R}{E_{\text{cm}}} \right]$$

$$\mathbf{s}_{\text{non-res}}(E_{\text{cm}}) = k * \mathbf{s}_{\text{DB}}(E_{\text{cm}})$$

where  $\mathbf{s}_{\text{DB}}(E_{\text{cm}})$  is the direct capture (cluster model) calculation of Descouvemont and Baye.

fit parameters:  $k, E_R, \Gamma_p(E_R), \Gamma_g(E_R)$

note: the  $J^P = 1^+$  M1 resonance doesn't interfere with the E1 direct capture background in the total cross section, so the partial cross sections can be added.

In stellar burning

light nuclei  $A < 12-14$  direct reactions usually dominate  
 $A > 16-20$  resonance reactions dominate  
 (resonances are mostly above threshold but can also be sub-threshold).

Direct reaction:

From Clayton

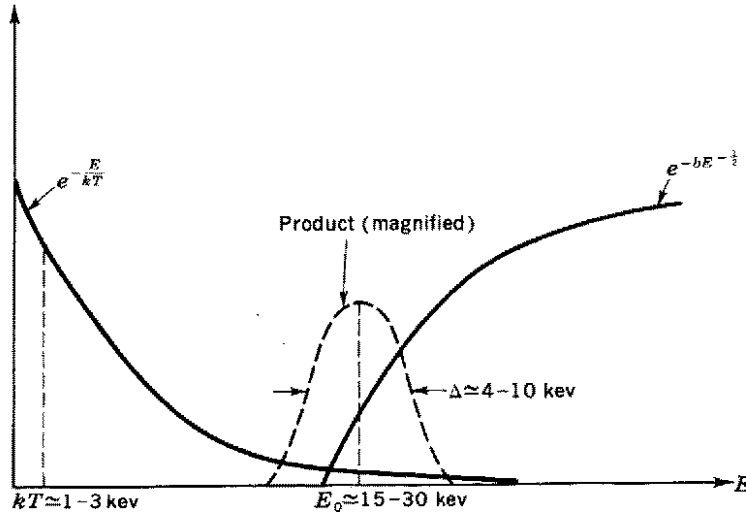


**Fig. 4-6** The dominant energy-dependent factors in thermonuclear reactions. Most of the reactions occur in the high-energy tail of the Maxwellian energy distribution, which introduces the rapidly falling factor  $\exp(-E/kT)$ . Penetration through the coulomb barrier introduces the factor  $\exp(-bE^{-1/2})$ , which vanishes strongly at low energy. Their product is a fairly sharp peak near an energy designated by  $E_0$ , which is generally much larger than  $kT$ . The peak is pushed out to this energy by the penetration factor, and it is therefore commonly called the *Gamow peak* in honor of the physicist who first studied the penetration through the coulomb barrier.

peak of Gamow window  $E_0$  :

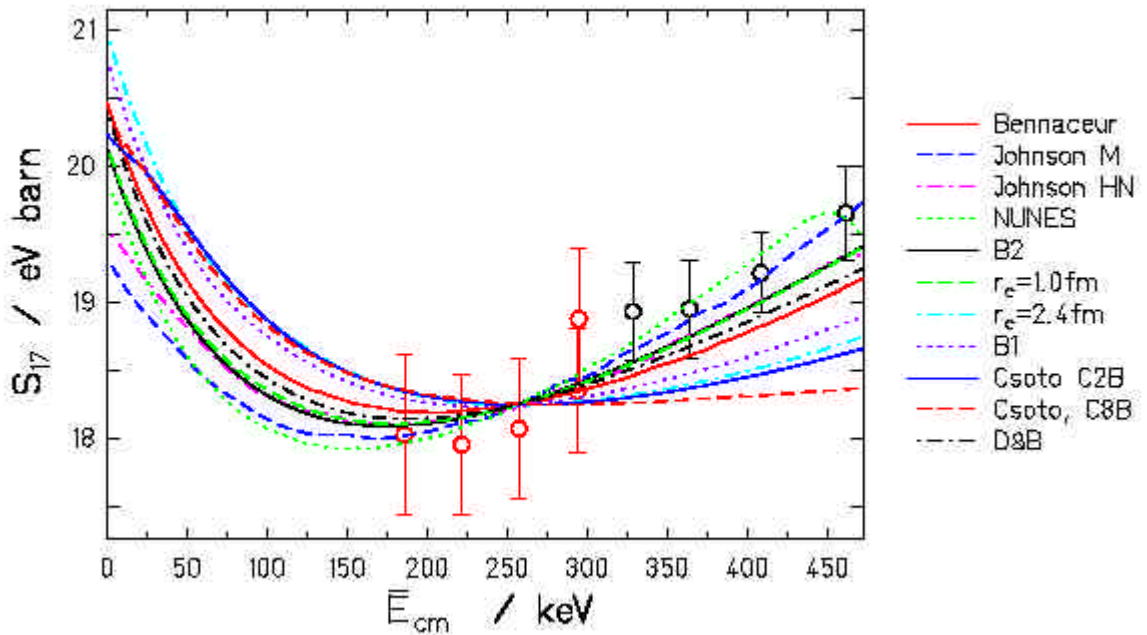
$$E_0 \cong \left( \frac{E_G kT}{2} \right)^2 = 1.220 \left[ Z_1^2 Z_2^2 \left( \frac{m}{M_n} \right) T_6^2 \right]^2 \text{ (keV)} \quad \text{where} \quad \frac{m}{M_n} = \frac{A_1 A_2}{A_1 + A_2}$$

$$= 18 \text{ keV for } {}^7\text{Be}+p. \quad (\text{Compare to } E_0(p-p) \cong 6 \text{ keV}).$$

width of Gamow window (full width at 1/e):

$$\Delta \cong \left( \frac{2E_G kT}{3} \right)^{1/2} = 11 \text{ keV for } {}^7\text{Be}+p.$$

# Extrapolation to $S_{17}(0)$

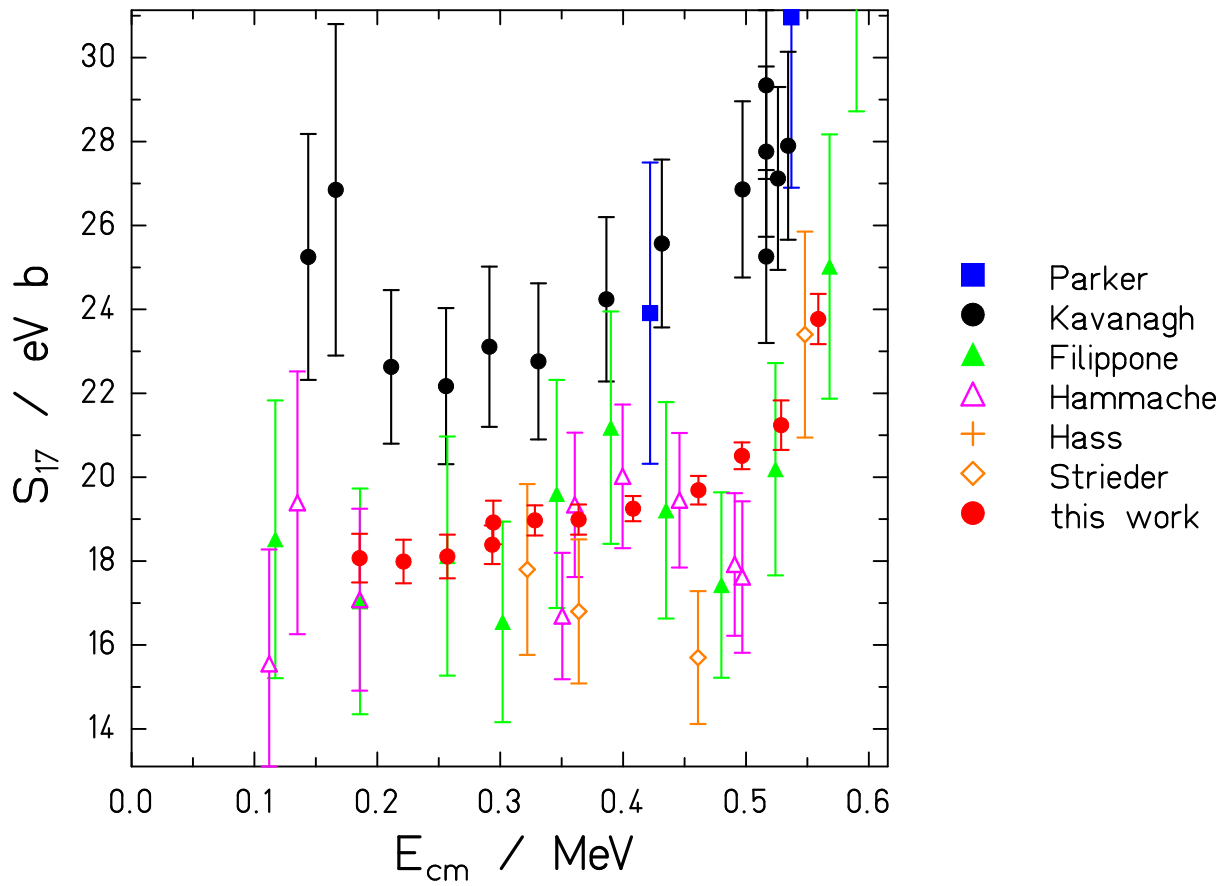


Fit with 11 different models to data  $E_{\text{cm}} < 300$  keV

- Standard deviation  $\sigma = 0.5$  eV-barn  
both from  $S_{17}(20)$  and  $S_{17}(0)$  distributions
- Central value from Descouvemont & Baye Model.  
(Best fit to our full data set.)

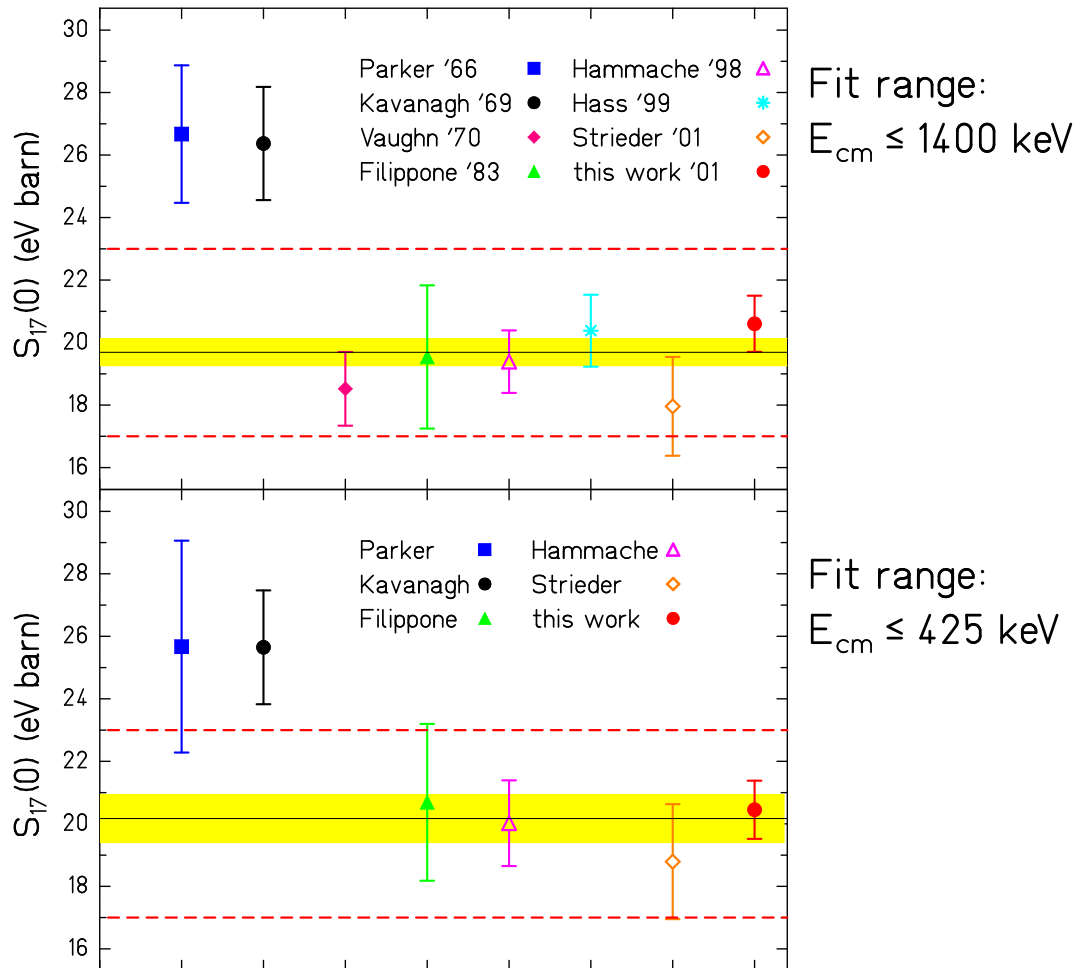
[Note: Jennings  $\Rightarrow \pm 0.2$  eV barn extrapolation error]

## Comparison of Experimental Data:



Kavanagh, Parker, Filippone renormalised with  $\sigma(^7\text{Li}(d,p)) = 152 \pm 6$  mbarn  
Scatter of data strongly reduced in this work.  
Parker, Kavanagh are systematically higher.

## Comparison of Experimental Results:

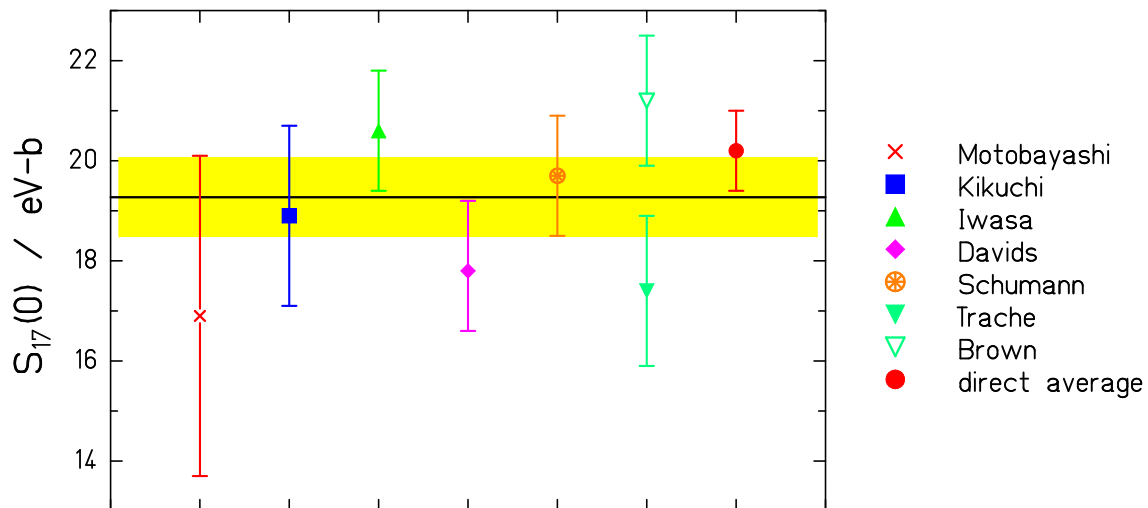


$E_{cm} \leq 425$  keV, Average  $S_{17}(0) = 20.2 \pm 0.8$  eV barn,  $\chi^2/\nu = 0.3$

Total error, including 2.2% extrapolation uncertainty

→Filippone, Hammache, Strieder, this work agree

## Indirect measurements:



**Yellow Band:** Mean of Coulomb dissociation results

**Red Point:** Average of 4 direct measurements

→ Good Agreement between direct and indirect methods

Coulomb dissociation:

Motobayashi et al., Phys. Lett. B 264 (1991) 259

Kikuchi et al., Eur. Phys. J. A 3 (1998) 209

Iwasa et al., Phys. Rev. Lett. 83 (1999) 2910

Davids et al., Phys. Rev. Lett. 86 (2001) 2750

Schumann et al., GSI Ann. Rep. 2001

Asymptotic Normalisation Coefficients (ANC):

Trache et al., Phys. Rev. Lett. 87 (2001) 271102

B.A. Brown et al., preprint - correction of Trache result

Source	Flux ( $10^{10} \text{ cm}^{-2}\text{s}^{-1}$ )	Cl (SNU)	Ga (SNU)
pp	$5.95 \times 10^0 \left(1.00^{+0.01}_{-0.01}\right)$	0.00	69.7
pep	$1.40 \times 10^{-2} \left(1.00^{+0.01}_{-0.01}\right)$	0.22	2.8
hep	$9.3 \times 10^{-7}$	0.04	0.1
$^7\text{Be}$	$4.77 \times 10^{-1} \left(1.00^{+0.09}_{-0.09}\right)$	1.15	34.2
$^8\text{B}$	$5.93 \times 10^{-4} \left(1.00^{+0.14}_{-0.15}\right)$	6.76	14.2
$^{13}\text{N}$	$5.48 \times 10^{-2} \left(1.00^{+0.19}_{-0.13}\right)$	0.09	3.4
$^{15}\text{O}$	$4.80 \times 10^{-2} \left(1.00^{+0.22}_{-0.15}\right)$	0.33	5.5
$^{17}\text{F}$	$5.63 \times 10^{-4} \left(1.00^{+0.12}_{-0.11}\right)$	0.00	0.1
Total		$8.59^{+1.1}_{-1.2}$	$130^{+9}_{-7}$

<Fractional uncertainty>	pp	$^3\text{He}^3\text{He}$	$^3\text{He}^4\text{He}$	$^7\text{Be} + p$	$Z/X$	opac	lum	age	diffuse	Total
	0.017	0.060	0.094	0.040	0.061		0.004	0.004	0.15	
Flux										
pp	0.002	0.002	0.005	0.000	0.004	0.003	0.003	0.0	0.003	0.009
$^7\text{Be}$	0.016	0.023	0.080	0.000	0.034	0.028	0.014	0.003	0.018	0.098
$^8\text{B}$	0.040	0.021	0.075	0.040	0.079	0.052	0.028	0.006	0.040	0.144 (0.175)
SNU <sub>s</sub>										
Cl	0.3	0.2	0.6	0.3	0.6	0.4	0.2	0.04	0.3	
Ga	1.3	1.0	3.3	0.6	3.1	1.8	1.3	0.20	1.5	

New  $S_{17}(0) = 20.2 \pm 0.8 \text{ eV-b}$   
(mean of 4 separate measurements)

Old  $S_{17}(0) = 19 + 4 - 2 \text{ eV-b}$

Neutrino mixings and oscillations  
- simple 2-state model

$$\mathbf{n}_e = \cos \mathbf{q} \cdot \mathbf{n}_1 + \sin \mathbf{q} \cdot \mathbf{n}_2$$

$$\mathbf{n}_m = -\sin \mathbf{q} \cdot \mathbf{n}_1 + \cos \mathbf{q} \cdot \mathbf{n}_2$$

$\mathbf{n}_1, \mathbf{n}_2$  mass eigenstates

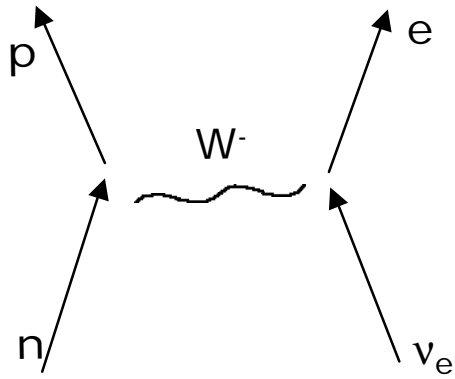
$\mathbf{n}_e, \mathbf{n}_m$  weak interaction (flavor) eigenstates

If neutrinos have mass, then:

$$P(\mathbf{n}_e \rightarrow \mathbf{n}_m) = \sin^2 2\mathbf{q} \cdot \sin^2 \left[ \frac{\Delta m^2 \cdot L}{4E_n} \right]$$

$$\mathbf{q} = \text{mixing angle}, \quad \Delta m^2 = m_2^2 - m_1^2$$

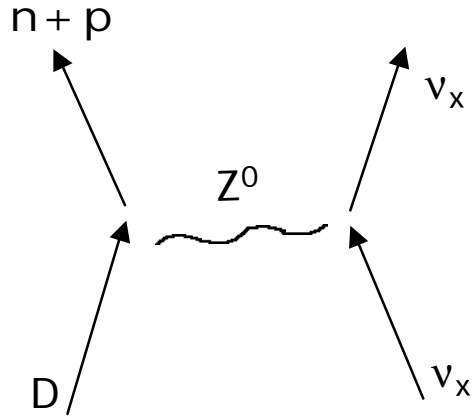
Sudbury Neutrino Observatory (SNO): Heavy water D<sub>2</sub>O



$$\nu_e + n \rightarrow p + e$$

$$\nu_e + D \rightarrow p + p + e$$

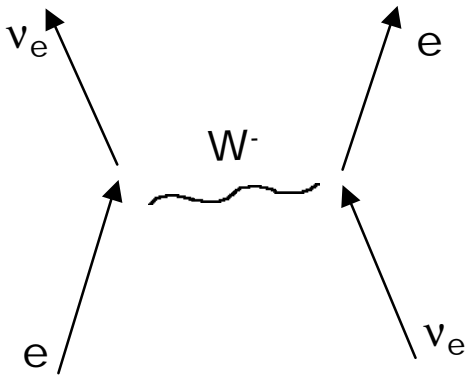
"charged current"



$$\nu_x + D \rightarrow n + p + \nu_x$$

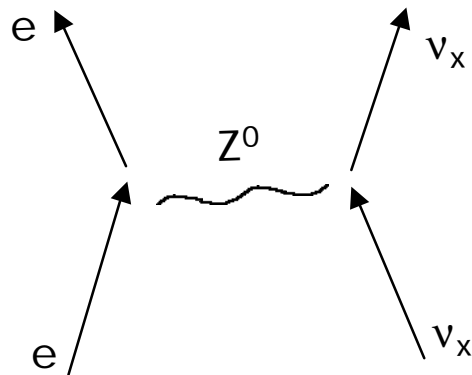
"neutral current"

Elastic scattering, SNO + Super-K:



$$\nu_e + e \rightarrow \nu_e + e$$

"charged current"



$$\nu_x + e \rightarrow \nu_x + e$$

$$\nu_x = \nu_e, \nu_\mu, \nu_\tau$$

"neutral current"

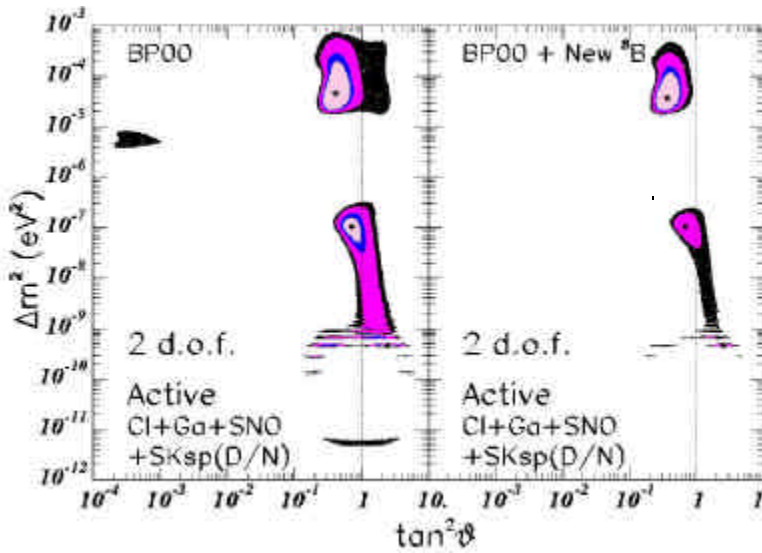
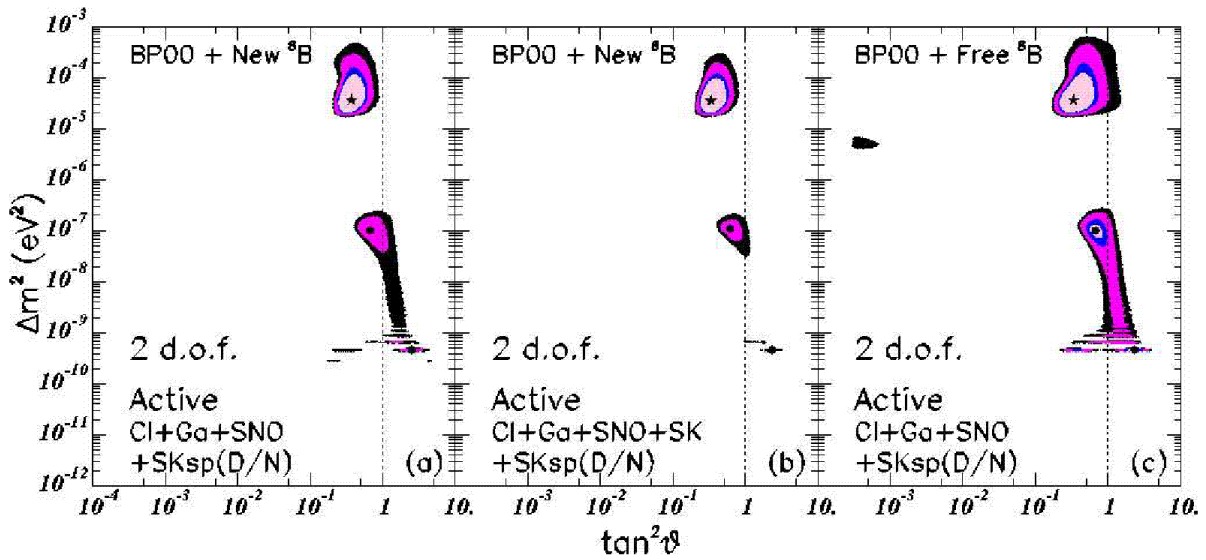
Rel. strength 1

1/6

SNO determines  $\nu_e$  flux and  $(\nu_\mu + \nu_\tau)$  flux separately



Allowed regions  $\leq 3\sigma$  (99.73% cL) 2-neutrino oscillation analysis



H. Schlattl et al.,  
Phys. Rev. D60, 113002 (1999)

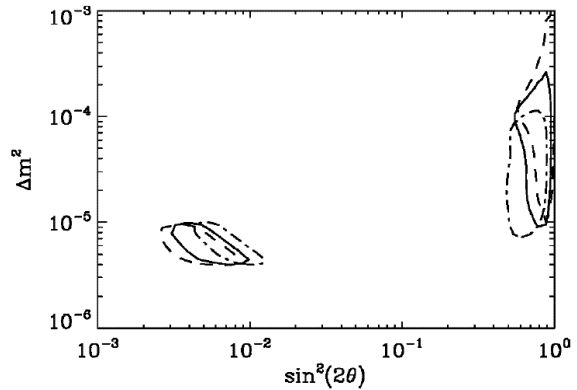


FIG. 3. Allowed regions (95% C.L.) of neutrino mixing parameters in a two flavor case for solar models with different cross sections of  ${}^7\text{Be}(p, \gamma){}^8\text{B}$  ( $S_{17}=17$  dashed line, 19 solid line and 23 dash-dotted line, in units of eV b).

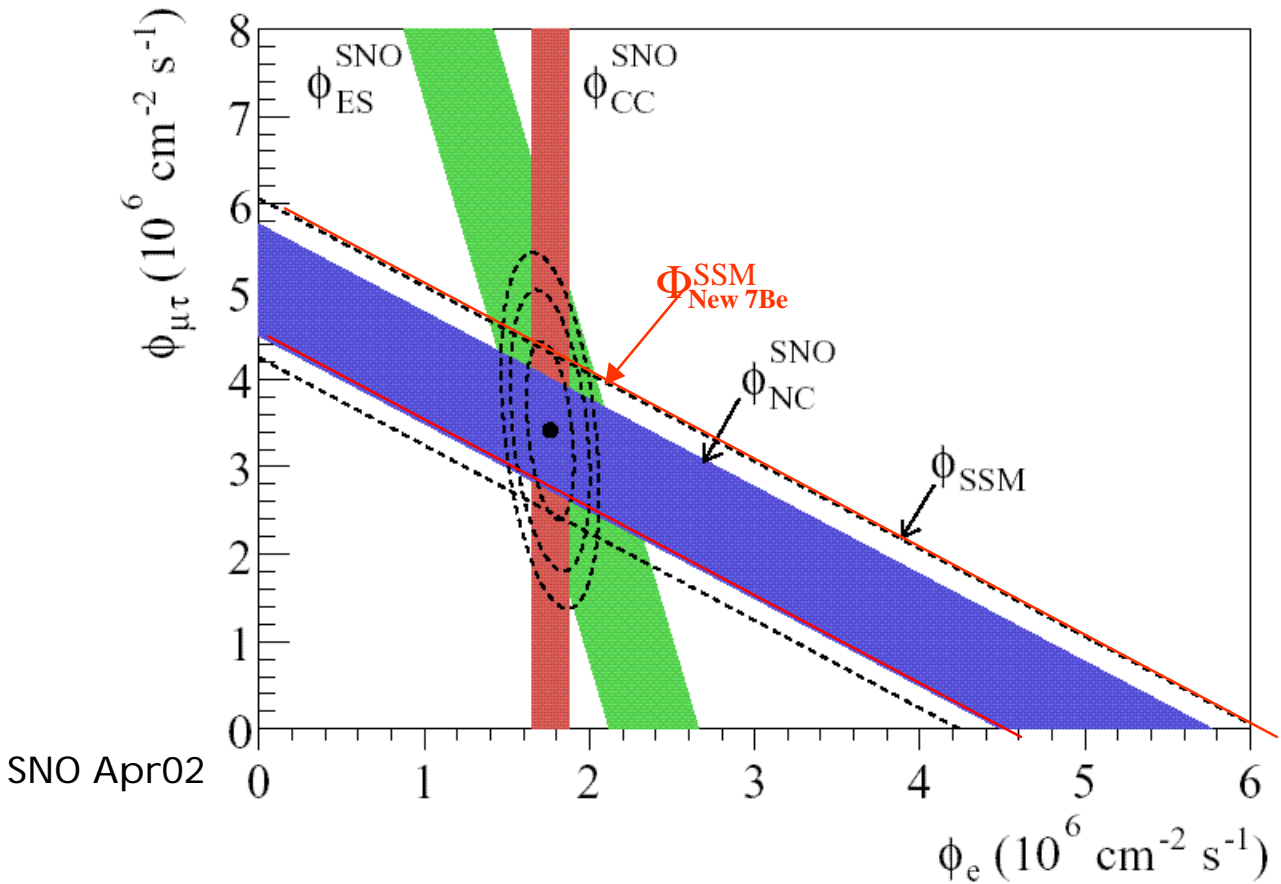
3 different neutrino oscillation experiments all see evidence for neutrino oscillations, with different values for  $\delta m^2$ :

			$\delta m^2$
Super-K	atmospheric	$\nu_\mu \rightarrow \nu_\tau$	$\sim 10^{-2} \text{ eV}^2$
SNO	solar	$\nu_e \rightarrow \nu_{\mu+\tau}$	$\sim 10^{-4} \text{ eV}^2$
LSND	accelerator	$\bar{\nu}_m \rightarrow \bar{\nu}_e$	$\sim 1 \text{ eV}^2$

3 distinct values of  $\delta m^2 \Rightarrow$  4 different neutrinos!

$\Rightarrow e, \mu, \tau$  and "sterile"

# Neutrino fluxes



$$\begin{aligned} \Phi_{SNO}^{CC}(v_e) &= 1.76 \pm 0.10 (\pm 6\%) \times 10^6 \text{ cm}^{-2} \text{ s}^{-1} \\ \Phi(v_\mu + v_\tau) &= 3.41 \pm 0.65 (\pm 19\%) \\ \Phi_{tot}(v_{active}) &= 5.09 \pm 0.62 (\pm 12\%) \text{ } (^8\text{B shape constr.}) \\ \Phi_{tot}(v_{active}) &= 6.42 \pm 1.67 (\pm 26\%) \text{ (unconstrained.)} \end{aligned}$$

$$\begin{aligned} \Phi_{New 7Be}^{SSM} &= 5.37 \pm 0.78 (\pm 14.5\%) \\ &\quad \text{(based on } S_{17}(0) = 20.2 \pm 0.8 \text{ eV-b)} \\ &= 5.05 \pm 0.89 (\pm 17.6\%) \\ &\quad \text{(based on } 19 + 4 - 2 \text{ eV-b)} \end{aligned}$$

new  $^7\text{Be}$ :

$$\begin{aligned} \Phi(v_s) / \Phi(v_\mu + v_\tau) &= +0.08 \pm 0.31 \leq 0.39(1\sigma), \leq 0.70(2\sigma) \\ \Phi(v_s) / \Phi(v_\mu + v_\tau) &= -0.23 \pm 0.32 \leq 0.09(1\sigma), \leq 0.42(2\sigma) \end{aligned}$$

## Conclusion

$S_{17}(0) = 20.2 \pm 0.8$  (expt + theor) eV-b  
mean of 4 modern direct measurements  
at low  $E_p$  below the resonance  
( including preliminary Seattle result)

Previously  $S_{17}(0)$  was largest error contribution to  $\phi^{\text{ssm}}(^8\text{B})$

With new results,  $S_{17}(0)$  uncertainty makes an unimportant contribution to  $\phi^{\text{ssm}}(^8\text{B})$

$\phi^{\text{ssm}}(^8\text{B})$  is still important for neutrino physics!

Comparison with SNO+ Super-K

⇒ tremendous vindication of SSM.

New “Phase II” measurements currently underway:

- 1) finalize absolute cross section
- 2) new data down to  $E_{\text{cm}} \approx 120$  keV